HHS Public Access

Author manuscript

J Immunol. Author manuscript; available in PMC 2019 May 01.

Published in final edited form as:

J Immunol. 2018 May 01; 200(9): 3128–3141. doi:10.4049/jimmunol.1701573.

Lipocalin 2 plays an important role in regulating inflammation in retinal degeneration

Tanu Parmar[†], **Vipul M Parmar**[†], **Lindsay Perusek**[†], **Anouk Georges**[§], **Masayo Takahashi**[§], **John W Crabb**[¶], and **Akiko Maeda**[†,‡,§]

[†]Department of Ophthalmology and Visual Sciences, Case Western Reserve University, Cleveland, OH 44106

[‡]Department of Pharmacology, Case Western Reserve University, Cleveland, OH 44106

[§]Laboratory for Retinal Regeneration, RIKEN Center for Developmental Biology, Kobe, Hyogo, 650-0047

[¶]Cole Eye Institute, Cleveland Clinic, OH 44195

Abstract

It has become increasingly important to understand how retinal inflammation is regulated because inflammation plays a role in retinal degenerative diseases. Lipocalin 2 (LCN2), an acute stress response protein with multiple innate immune functions, is increased in *Abca4*$^{-/-}$*Rdh8*$^{-/-}$ double knockout mice, an animal model for Stargardt disease and age-related macular degeneration (AMD). To examine roles of LCN2 in retinal inflammation and degeneration, *Lcn2*$^{-/-}$*Abca4*$^{-/-}$*Rdh8*$^{-/-}$ triple knockout mice were generated. Exacerbated inflammation following light exposure was observed in *Lcn2*$^{-/-}$*Abca4*$^{-/-}$*Rdh8*$^{-/-}$ mice as compared with *Abca4*$^{-/-}$*Rdh8*$^{-/-}$ mice, with upregulation of pro-inflammatory genes and microglial activation. RNA array analyses revealed an increase in immune response molecules such as *Ccl8*, *Ccl2* and *Cxcl10*. To further probe a possible regulatory role for LCN2 in retinal inflammation, we examined the *in vitro* effects of LCN2 on NF-κB signaling in human retinal pigmented epithelial (RPE) cells differentiated from induced pluripotent stem cells (hiPS-RPE) derived from healthy donors. We found that LCN2 induced expression of antioxidant enzymes HMOX1 and SOD2 in these RPE cells and could inhibit the cytotoxic effects of H_2O_2 and lipopolysaccharide. Enzyme-linked Immunosorbent Assay revealed increased LCN2 levels in plasma of patients with Stargardt disease, retinitis pigmentosa and AMD as compared with healthy controls. Finally, overexpression of *LCN2* in RPE cells displayed protection from cell death. Overall these results suggest that LCN2 is involved in pro-survival responses during cell stress and plays an important role in regulating inflammation during retinal degeneration.

Keywords

Rodent model; human iPS cells; retinal degeneration; acute phase proteins; inflammation; knockout mice; retina

To whom correspondence should be addressed: Akiko Maeda, Department of Ophthalmology and Visual Science, Case Western Reserve University, 10900 Euclid Ave., Cleveland, OH 44106. Tel.: 216-368-0670; Fax; 216-368-3171; aam19@case.edu.

Introduction

Several blinding diseases of the retina are characterized by the death of RPE and photoreceptor cells. In retinitis pigmentosa (RP), an inherited retinal disease characterized by a progressive loss of photoreceptor cells, an activation of pro-survival signaling cascades, involving upregulation of several growth factors, cytokines and antioxidants, has been observed (1). In age-related macular degeneration (AMD), a major cause of visual impairment in elderly people, several immune responses are activated in the form of inflammatory cytokines, chemokines, antibodies, and T cells in both animal models and patients (2). Accumulating evidence suggests that activation of immune responses plays an important role in progression of these blinding diseases. We previously reported an increase in acute phase protein Lipocalin 2 (LCN2) coinciding with retinal degeneration in *Abca4*$^{-/-}$*Rdh8*$^{-/-}$ mice (3). LCN2 is also known as 24p3 or neutrophil gelatinase-associated lipocalin (NGAL) and is a member of the lipocalin superfamily known for its role in cellular transport of lipophilic molecules as fatty acids, iron, retinoids and steroids. LCN2 is a multifunctional innate immunity protein and can augment cellular tolerance to oxidative stress (4) and indeed, roles of LCN2 have been suggested under stress conditions and degenerative diseases. In the central nervous system, LCN2 deficiency has been associated with tissue inflammation (5). *Lcn2* deficient mice were found to be highly sensitive to bacterial sepsis (6). Several studies have demonstrated that LCN2 protects against cellular stress, inflammation and cell death (7–10).

Although a few studies have implicated the involvement of LCN2 in eye disease, the possible roles of LCN2 in retinal degeneration have not been fully elucidated. LCN2 was found upregulated amongst other acute phase response and inflammatory proteins in the retina of rodent models for diabetes and retinal ischemia-reperfusion injury (11). Increased levels of LCN2 have been reported in a mouse model of Bardet-Biedl Syndrome (12). A pivotal role of LCN2 in the development of demyelinating optic neuritis in a mouse model of autoimmune optic neuritis (EAON) has been demonstrated (13). Valapala et al identified LCN2 as a contributory factor in inducing chronic inflammatory response in *Cryba1* conditional knockout mice, a mouse model with AMD-like pathology (14). Lastly, Sinha et al generated genetically engineered mice in which lysosome-mediated clearance in RPE cells is compromised, causing the development of features of early AMD (15). They further proposed the involvement of an AKT2-NF-κB-LCN2 signaling axis in activating the inflammatory responses in these mice, suggesting this pathway as a potential target for AMD treatment. In humans, Ghosh et al observed an increased infiltration of LCN2-positive neutrophils in the choroid and retina of early AMD patients as compared with age-matched controls (15). These studies including our observation of increased expression of LCN2 in mouse retinal degeneration (3), reinforce the possible significance of LCN2 in retinal inflammation and retinal degenerative diseases.

In the current study, *Lcn2*$^{-/-}$*Abca4*$^{-/-}$*Rdh8*$^{-/-}$ triple knockout mice were generated and human RPE cells differentiated from induced pluripotent stem cells (hiPS-RPE) were employed to investigate the role of LCN2 in retinal inflammation and degeneration. Our

results provide evidence that LCN2 could regulate pro-survival responses and retinal inflammation in mice and humans.

Materials and Methods

Animals

Lcn2$^{-/-}$ mice were purchased from Jackson Laboratory (Bar Harbor, ME). All the mice were housed in the animal facility at the School of Medicine, Case Western Reserve University, where they were maintained either under complete darkness or in a 12-h light (~10 lux)/12-h dark cycle environment in a pathogen-free environment. Both male and female mice at 1 month of age were used in the study. *Lcn2*$^{-/-}$ mice were crossed with *Abca4*$^{-/-}$*Rdh8*$^{-/-}$ mice to generate *Lcn2*$^{-/-}$*Abca4*$^{-/-}$*Rdh8*$^{-/-}$ mice. 129SV or littermates of mutant mice were used as controls. Only the mice with RPE65 leucine variant and free of *rd8* mutation were employed in the study. Genotyping for *Lcn2*$^{-/-}$ or WT mice was performed using the primers with LCN2-KO and common for KO allele and LCN2-WT and common for WT allele; LCN2-KO: 5′-CCTTCTAT GCCTTCTTGACG-3′, LCN2-common: 5′-TAGGGGATGCCACATCTCA-3′, LCN2-WT: 5′-TGGAGGTGACATTGTAGCTATTG-3′. Genotyping for *Abca4*$^{-/-}$*Rdh8*$^{-/-}$ mice was performed as described previously (16). All animal procedures and experiments were approved by the Case Western Reserve University Animal Care Committees and conformed to recommendations of both the American Veterinary Medical Association Panel on Euthanasia and the Association of Research for Vision and Ophthalmology.

Light exposure

Mice were dark-adapted for 48 h before being exposed to light. Light-induced degeneration was induced by exposing mice to 10,000 lux of diffuse white fluorescent light (150 W spiral lamp; Commercial Electric, Cleveland, OH) for 30 min. Before such light exposure, pupils of mice were dilated with mixture of 0.5% tropicamide and 0.5% phenylephrine hydrochloride (Midorin-P®, Santen Pharmaceutical Co., Ltd., Osaka, Japan). After exposure animals were kept in the dark until further evaluation.

Histological Analysis

All procedures to make sections for retinal histology and immunohistochemistry followed established methods (17, 18). For hematoxylin-eosin staining eye cups were fixed in 10% formalin for 72 h followed by paraffin embedding. Five μm thick sections were cut and stained with hematoxylin-eosin for analysis by light microscopy. For immunohistochemistry eye cups were embedded in 4% paraformaldehyde, 1% glutaraldehyde overnight followed by cryosectioning. The following antibodies were used for immunohistochemistry; rabbit anti-Iba-1 Ab (1:400, Wako, Chuo-ku, Osaka, Japan), rabbit anti-Glial Fibrillary Acidic Protein Ab (1:400, Dako, Carpinteria, CA), rabbit NF-kB p65 Ab (1:1000, eBioscience™, San Diego, CA). Secondary antibodies used were anti-mouse, anti-rabbit Alexa 555 (Invitrogen, Carlsbad, CA). Images were captured by a confocal microscope (LSM, Carl Zeiss, Thornwood, NY).

Scanning laser ophthalmoscopy (SLO) and spectral domain-optic coherence tomography (SD-OCT) imaging

HRAII (Heidelberg Engineering, Heidelberg, Germany) for SLO, and ultra-high resolution SD-OCT (Bioptigen SD-OCT Envisu C2200; Bioptigen, Research Triangle Park, NC, USA) were employed for *in vivo* imaging of mouse retinas. Mice were anesthetized by intraperitoneal injection of a mixture (20 μl/g body weight) containing ketamine (6 mg/ml) and xylazine (0.44 mg/ml) in 10 mM sodium phosphate, pH 7.2, with 100 mM NaCl. Pupils were dilated with mixture of 0.5% tropicamide and 0.5% phenylephrine hydrochloride (Midorin-P®, Santen Pharmaceutical Co., Ltd). Numbers of autofluorescent (AF) particles in SLO images were counted per image.

Quantitative RT-PCR (qRT-PCR)

Total RNA was extracted with the RNeasy Mini Kit (Qiagen, Germantown, MD). Primers used in the study have been listed in supplemental Table 1. All procedures for qRT-PCR were carried out as described previously (19).

Immunoblot

Enucleated eyes were harvested from the animals and lysed in ice-cold lysis buffer (150 mM NaCl, 1 mM EDTA, 0.2% Nonidet P-40 and 20 mM Tris-HCl, pH 7.5) containing protease inhibitor mixture (Sigma-Aldrich, St. Lois, MO). Tissue lysate was spun at 10,000 rpm for 10 min at 4 °C. Proteins from each sample were transferred onto Immobilon-P membranes (Millipore, Bedford, MA) after SDS-PAGE gel electrophoresis. Membranes were incubated in 1% BSA solution containing a 1:1000 dilution of either anti-LCN2 rabbit polyclonal antibody (sc-50350, Santa Cruz Biotechnology, Santa Cruz, CA) or anti-β-actin antibody (Santa Cruz Biotechnology). Signals were visualized with alkaline phosphatase (Promega, Madison, WI) at a dilution of 1: 10000. The intensities of the bands were normalized to the actin band using Image J software (National Institute of Health, Bethesda, MD).

Isolation of primary RPE and microglia cells

Primary mouse RPE cells and retinal microglial cells were prepared from 2-week-old mice based on previously published methods (19, 20). Enucleated eyes were incubated with 2% dispase (Invitrogen) in Dulbecco's modified Eagle's medium (DMEM) (Invitrogen) for 1 h at 37 °C, and neural retinas and eyecups were separated under a surgical microscope (ILLUMIN-i, Endure Medical, Cumming, GA). The RPE layer was peeled from eye cups, and cultured in DMEM containing minimal essential medium non-essential amino acids (Invitrogen), penicillin/streptomycin (Invitrogen), 20 mM HEPES, pH 7.0, and 10% fetal bovine serum. To enrich microglial cells, neural retinas were homogenized and cultured in DMEM containing minimal essential medium non-essential amino acids (Invitrogen), penicillin/streptomycin (Invitrogen), 20 mM HEPES, pH 7.0, and 10% fetal bovine serum for 7 days at 37 °C. Adherent cells to the plastic surface were treated with 0.05% trypsin (Invitrogen), and less adhesive cells were collected as microglial cells. Human primary RPE cells were purchased from Lonza (Walkersville, MD).

Stimulation with photoreceptor outer segment (POS) and lipopolysaccharide (LPS)

POS membranes were prepared from 1-month-old *Abca4*$^{-/-}$*Rdh8*$^{-/-}$ and WT mice using a published method (19). LPS was purchased from Invivogen (San Diego, CA).

hiPS-RPE cell culture

Establishment of hiPS cell lines and differentiated to RPE monolayers has been described in detail (21–25). All procedures were approved by the Institutional Review Boards at the Case Western Reserve University, Cleveland Ohio and adhered to the Declaration of Helsinki. All cell culture procedures were approved by Case Western Reserve University Institutional Biosafety Committee. All samples were obtained after donors had given informed consent.

Apoptosis assay

hiPS-RPE cells (30,000–50,000) were seeded in 96 well plates. Cells were treated with 100 μM H_2O_2 and recombinant LCN2 protein (R&D Systems, Minneapolis, MN) in doses of 1, 10, 100 ng/ml for 24 h. Next day 1 drop/ ml of CellEvent™ Caspase 3/7 Green Detection Reagent was added to each well for 60 min at 37 °C. Cells were then washed and fixed in 4% paraformaldehyde for 15 min, followed by 4′,6′-diamidino-2-phenylindole (DAPI) staining. Cells were visualized and imaged under inverted fluorescence microscope.

Cell viability assay

Assay was performed on 96-well plates, with $1x10^4$ cells seeded in each well. Cells were incubated with and without recombinant LCN2 (R&D Systems) for 24 h. After 2 h incubation, 10 μl of the WST-1 solution (Roche, CA) were added to the culture medium and incubated for 2 h at 37 °C. Absorbance was measured using a microplate ELISA reader (Multiscan FC Microplate Reader, Fisher Scientific Inc., Pittsburgh, PA). All experiments were conducted in triplicate and replicated at least three times. Viable cells number was calculated by comparing the absorbance values of the samples after background subtraction.

Enzyme-linked Immunosorbent Assay (ELISA)

Amounts of CCL2, TNFα and LCN2 in serum, plasma and tissue homogenates were quantified by ELISA kits (R&D System) according to manufacturer's instructions. Eyes were homogenized in 500 μl of Nonidet P-40 lysis buffer containing 20 mM Tris, pH 8.0, 137 mM NaCl, and 1% Nonidet P-40. Protein concentrations were measured using a NanoDrop (Thermo Fisher Scientific, Waltham, MA).

RNA array analysis

Detection and quantification of gene expression was performed using a Mouse Inflammatory Cytokine and Receptors array (PAMM-011ZF; SABiosciences/QIAGEN, Frederick, USA) according to the manufacturer's instructions. This PCR based array was selected as it includes 84 diverse genes important in the immune response, including genes encoding CC chemokines, CXC chemokines, interleukin cytokines, other cytokines, chemokine receptors, and cytokine receptors, as well as other genes involved in the inflammatory response. microRNA (miRNA) array was also performed using an Inflammatory Response miRNA PCR Array (MIMM-105Z; SABiosciences/QIAGEN) according to the manufacturer's

instructions. Real-time PCR amplification was performed using RT^2 SYBR Green PCR Master Mix (QIAGEN). Primers were designed using web tool Primer 3 and synthesized by Eurofins MWG Operon (Huntsville, AL). Data analysis was performed using the $\Delta\Delta C_T$ method according to the manufacturer's protocol (SABiosciences).

Immunocytochemistry for NF-κB localization

hiPS-RPE cells (30,000–50,000) were seeded in 96 well plates. Cells were co-incubated with 1 μg/ml of LPS and 1 ng/ml of LCN2 for 24 h. Next day the culture medium was removed and cells were fixed by adding 100 μl of 4% formalin to the wells for 15 min, followed by washing in PBS twice for 5 min. Fixed cells were permeabilized with 100 μl of 0.2% Triton X-100 in PBS for 1 min at room temperature. The cells were then incubated with rabbit anti-mouse p65 (1:100 (eBioscience Ltd) in PBS containing 10% goat serum overnight at 4°C. Cells were then washed twice with PBS and incubated with Alexa Fluor 488-labeled goat anti-rabbit IgG antibody (1:200) (Molecular Probes Inc.) in PBS at room temperature for 2 h. The cells were washed twice for 5 min with PBS. DAPI (1: 500; Vector Laboratories, UK) was added to the cells to visualize the nuclei. Cells were then washed twice with PBS and imaged under fluorescent microscope. Five high power fields (× 100 magnifications) were randomly selected in each sample for analysis. Positive nuclear staining in LPS treated cells was used as positive control for NF-κB staining. The percent of nuclear staining for NF-κB p65 was scored by counting the positive-stained cells and the total number of cells quantified in random microscopic fields using the Metamorph image analysis software (Molecular Devices, San Jose, CA).

Measurement of NF-κB Activity by ELISA

hiPS-RPE cells (30,000–50,000) were seeded in 96 well plates. Cells were co-incubated with 1 μg/ml of LPS and 1 ng/ml of LCN2 for 24 h. Next day media was removed and cells were rinsed once with ice-cold PBS. Next PBS was removed and 100 μl of Nonidet P-40 lysis buffer was added and incubated the plate on ice for 5 min. Scraped off the cells followed by centrifugation for 10 min (x 14,000 rpm) at 4°C. Supernatant was collected and total protein was measured using a Nanodrop (Thermo Fisher Scientific). Total endogenous levels of total NF-κB p65 protein was then measured using the PathScan® total NF-κB p65 sandwich ELISA Kit (#7174; Cell Signaling Technology, Danvers, MA) according to the manufacturer's instruction. Endogenous levels of phospho-NF-κB p65 protein were measured using the PathScan® Phospho-NF-κB p65 sandwich ELISA Kit (#7173; Cell Signaling Technology) according to the manufacturer's instructions. ELISA results were normalized to the total protein content per well.

Human plasma analysis

All the participants in the study underwent a complete ophthalmic examination and visual function tests by ophthalmologists. Informed consent was obtained from each person for the present study. Procedures followed the Declaration of Helsinki guidelines and were approved by the Institutional Review Boards of Case Western Reserve University, RIKEN, Institute of Biomedical Research and Innovation Hospital and Cleveland Clinic. Nonfasting blood samples were collected at the Institute of Biomedical Research and Innovation Hospital or at the Cole Eye Institute from patients diagnosed with Stargardt disease (n=11),

RP (n=117) and wet form of AMD (n = 57). Blood was also collected from healthy controls (n=77) who had no retinal degeneration as determined by ophthalmologic examination. Healthy controls include family members of patients with inherited retinal disorder and individuals who underwent cataract surgery. Plasma was prepared as previously described and stored under argon at −80 °C until analysis (26).

Overexpression of LCN2 in ARPE19 cells

pcDNA3.1-LCN2 (OHu27037D) was purchased from GeneScript USA Inc. (Piscataway, NJ). ARPE19 cells (American Type Culture Collection (ATCC), Manassas, VA) were transiently transfected with 1 μg of pcDNA3.1-LCN2 or pcDNA3.1 plasmids using Lipofectamine 3000 (ThermoFisher Scientific) according to the manufacturer's protocol. Expression of *LCN2* mRNA was then examined by RT-PCR 72 h after transfection using primers shown in supplemental Table 1.

Statistical analysis

Statistical analyses were performed using the t-test for comparing 2 groups, and one-way ANOVA was used to detect differences among 3 or more groups. Mann-Whitney U Statistics were employed to analyse human plasma samples. Results were presented as mean ± SD. The results were considered statistically significant at $P < 0.05$.

Results

Increased expression of Lcn2 in the retina and brain after light exposure

To examine expressional changes of acute stress protein LCN2 in various tissues under stress conditions which can induce retinal degeneration, 1-month-old *Abca4*$^{-/-}$*Rdh8*$^{-/-}$ mice were exposed to light at 10,000 lux for 30 min and qRT-PCR was performed with isolated tissues including the eye, liver, heart, brain, spleen, lung and kidney. Two-fold or higher increase of *Lcn2* was observed in the eye (15.38±3.86) and brain (4.97±0.55) when compared with dark adapted controls (Fig. 1A). *Lcn2* expression was not obvious in these tissues prior to light exposure except spleen where low levels of *Lcn2* expression were detected. To determine the kinetics of LCN2 levels in the eye after light exposure, LCN2 expression was examined by immunoblot 1, 3 and 7 days post illumination at 10,000 lux for 30 min. LCN2 protein in the eye was found most upregulated 1 day after light exposure (Fig. 1B, 1C). Greatest LCN2 increase in serum was observed 3 days after light exposure in mice (Fig. 1D). Immunohistochemistry indicated that secreted LCN2 protein was detected in RPE and microglial cells in the inner nuclear layer of the retina (Fig. 1E). Since incubation with photoreceptor outer segment proteins (POS) can induce production of inflammatory cytokines and chemokines from RPE and microglial cells (19), RPE and microglia cells were isolated from 2-week-old *Abca4*$^{-/-}$*Rdh8*$^{-/-}$ mice. When these cells were incubated with POS for 24 h, 14-fold or 5-fold increase in *Lcn2* was observed in RPE or microglial cells respectively (Fig. 2).

Deficiency of Lcn2 results in severe light-induced retinal degeneration in Abca4$^{-/-}$Rdh8$^{-/-}$ mice

To examine effects of *Lcn2* deficiency in retinal degeneration, 1-month-old *Lcn2*$^{-/-}$*Abca4*$^{-/-}$*Rdh8*$^{-/-}$ and *Abca4*$^{-/-}$*Rdh8*$^{-/-}$ mice were exposed to light at 10,000 lux for 30 min. WT littermates were subjected to the same light exposure. Histology sections of the retina demonstrated decrease in ONL thickness in *Lcn2*$^{-/-}$*Abca4*$^{-/-}$*Rdh8*$^{-/-}$ mice as compared with *Abca4*$^{-/-}$*Rdh8*$^{-/-}$ mice 7 days after light exposure (Fig. 3A upper panels, 3B). *In vivo* imaging of the retina by scanning laser ophthalmoscopy (SLO) was performed 7 days after light exposure (Fig. 3A lower panels). Increased number of autofluorescent (AF) spots, which are activated microglial cells and macrophages (19) were counted in *Lcn2*$^{-/-}$*Abca4*$^{-/-}$*Rdh8*$^{-/-}$ mice as compared with *Abca4*$^{-/-}$*Rdh8*$^{-/-}$ mice (Fig. 3C). *Lcn2*$^{-/-}$ mice did not develop light-induced retinal degeneration (see below section of "*Deficiency of Lcn2 is associated with inflammatory changes*").

Lcn2$^{-/-}$Abca4$^{-/-}$Rdh8$^{-/-}$ mice show stronger gliosis than Abca4$^{-/-}$Rdh8$^{-/-}$ mice after light exposure

In order to investigate effects of *Lcn2* deficiency to retinal glial cells after light exposure, we examined the expression of Iba-1 for microglial cells and GFAP for Müller cells. Activation of glial cells is associated with retinal inflammation (27). *Lcn2*$^{-/-}$*Abca4*$^{-/-}$*Rdh8*$^{-/-}$ and *Abca4*$^{-/-}$*Rdh8*$^{-/-}$ mice at 1 month of age were exposed to light at 10,000 lux for 30 min, and eyes were collected 24 h thereafter. Immunohistochemistry with anti-Iba-1 antibody showed increased protein expression and more Iba-1 positive microglial cell numbers in *Lcn2*$^{-/-}$*Abca4*$^{-/-}$*Rdh8*$^{-/-}$ mice as compared to *Abca4*$^{-/-}$*Rdh8*$^{-/-}$ mice (Fig. 4A upper panels). Immunohistochemical staining with anti-GFAP antibody revealed stronger gliosis with an increased expression of GFAP in Müller cells of *Lcn2*$^{-/-}$*Abca4*$^{-/-}$*Rdh8*$^{-/-}$ mice (Fig. 4A lower panels). qRT-PCR of *Gfap* displayed a similar pattern of increase as observed in immunohistochemistry (Fig. 4B). These results indicate that *Lcn2* deficiency contributes to stronger response of retinal glial cells which are associated with retinal inflammation.

Increased expression of inflammatory response in Lcn2$^{-/-}$Abca4$^{-/-}$Rdh8$^{-/-}$ mice

To further dissect LCN2 mediated effects on inflammatory genes and immune pathways, we employed the RT^2 real-time PCR array kit for 84 key immune genes involved in mediating inflammation. *Lcn2*$^{-/-}$*Abca4*$^{-/-}$*Rdh8*$^{-/-}$ and *Abca4*$^{-/-}$*Rdh8*$^{-/-}$ mice (1-month-old) were exposed to light at 10,000 lux for 30 min. Dark adapted mice were used for controls. The PCR array was performed 1 day (24 h) after light exposure. Total RNA was isolated from all groups of mice. Equal amounts were converted to cDNA and then subjected to pathway-focused gene expression profiling using real-time PCR. Scatter plots comparing the differential expression of genes in light exposed *Lcn2*$^{-/-}$*Abca4*$^{-/-}$*Rdh8*$^{-/-}$ and *Abca4*$^{-/-}$*Rdh8*$^{-/-}$ mice were generated (Fig. 5A). Each symbol represents an individual gene. The boundary lines indicate a 2-fold difference. Genes outside the boundary lines have ≥2-fold altered expression in *Lcn2*$^{-/-}$*Abca4*$^{-/-}$*Rdh8*$^{-/-}$ mice compared with *Abca4*$^{-/-}$*Rdh8*$^{-/-}$ mice. Table 1 lists the fold changes of the genes compared in the two groups of mice. *Lcn2*$^{-/-}$*Abca4*$^{-/-}$*Rdh8*$^{-/-}$ mice displayed upregulation of 22 inflammatory mediators including chemokines, chemokine receptors and interleukins as compared with

Abca4$^{-/-}$*Rdh8*$^{-/-}$ mice. Conversely, *Cx3cl1*, *Vegfa* and *Cxcl15* were downregulated in *Lcn2*$^{-/-}$*Abca4*$^{-/-}$*Rdh8*$^{-/-}$ mice. Validation by qRT-PCR for *Ccl8*, *Ccl2*, *Cxcl10*, *Ccr5*, *Tnf* and *Il2a* was carried out using a separate set of mice (Fig. 5B). Production of CCL2 and TNF was quantified with eyes of 1-month-old *Lcn2*$^{-/-}$*Abca4*$^{-/-}$*Rdh8*$^{-/-}$ and *Abca4*$^{-/-}$*Rdh8*$^{-/-}$ mice 24 h after light exposure at 10,000 lux for 30 min. Increased levels of CCL2 and TNF (34.75±1.5 pg/ml, TNF 6.02±0.04 pg/ml) in *Lcn2*$^{-/-}$*Abca4*$^{-/-}$*Rdh8*$^{-/-}$ mice compared to (CCL2 5.75±0.7pg/ml, TNF 1.26±0.02 pg/ml) in *Abca4*$^{-/-}$*Rdh8*$^{-/-}$ mice were measured (Fig. 5C, 5D).

Deficiency of Lcn2 is associated with inflammatory changes caused by light exposure

Since *Lcn2*$^{-/-}$*Abca4*$^{-/-}$*Rdh8*$^{-/-}$ mice displayed more severe light-induced retinal degeneration and inflammation as compared with *Abca4*$^{-/-}$*Rdh8*$^{-/-}$ mice (Figs. 3, 4 and 5), roles of LCN2 in retinal inflammation after light exposure were examined using *Lcn2*$^{-/-}$ mice. When 6-week-old *Lcn2*$^{-/-}$ mice were exposed to light at 10,000 lux for 30 min, increased levels of inflammatory changes were observed 24 h after illumination as compared with WT mice, including increased expression of *Iba-1*/*Aif-1* and *Gfap* (Fig. 6A). Though increased immune reactions were observed in *Lcn2*$^{-/-}$ mice, this light condition did not cause obvious retinal degenerative changes in *Lcn2*$^{-/-}$ and WT mice in contract that *Abca4*$^{-/-}$*Rdh8*$^{-/-}$ mice showed retinal structural changes 7 days after illumination (Fig. 6B). No retinal degeneration was observed in 6-week- and 4-month old *Lcn2*$^{-/-}$ mice when they were kept under regular lighting conditions. Because inflammatory changes in light-exposed *Lcn2*$^{-/-}$ mice suggest regulatory roles of LCN2 in inflammation, expression of miRNA which can modulate transcriptional expression of inflammatory molecules was examined by miRNA array. Changes in miRNA expression obtained from *Lcn2*$^{-/-}$ and WT mice are presented in Table 2. These results indicate that loss of *Lcn2* is prone to accelerating inflammation.

LCN2 attenuates LPS stimulated NF-κB activation in RPE cells

The LCN*2* gene promoter region contains binding sites for several transcription factors including NF-κB (28), which prompted us to examine the effects of LCN2 on NF-κB signaling in RPE cells. Notably, the nuclear factor NF-κB pathway is a prototypical pro-inflammatory signaling pathway involved in the expression of multiple pro-inflammatory genes such as cytokines, chemokines, and adhesion molecules (29–32). Human RPE cells differentiated from induced pluripotent stem cells (hiPS-RPE) were incubated with 1 μg/ml of LPS for 24 h to investigate whether LCN2 can inhibit the nuclear translocation of NF-κB p65. Immunocytochemistry with anti-p65 antibody revealed that LPS-stimulated hiPS-RPE cells showed p65 staining in the nuclei, while unstimulated cells showed stronger staining in the cytoplasm. Supplementation of LCN2 in the culture medium decreased the numbers of cells with LPS-induced nuclear translocation of p65 (Fig. 7A, 7B). Furthermore, phosphorylation of NF-κB p65, which indicates activation of NF-κB, was examined using ELISA. In contrast that levels of total NF-κB p65 remained unchanged, decrease in phosphorylated NF-κB p65 was observed when LCN2 was supplemented to hiPS-RPE cells (Fig. 7C). These observations suggest that LCN2 contributes to inhibition of NF-κB activation in human RPE cells. hiPS-RPE cells can express LCN2 as well as murine RPE cells when these cells were incubated with POS (supplemental Fig. 1).

LCN2 protects against oxidative stress by increasing the expression of antioxidant enzymes HMOX1 and SOD2 in hiPS-RPE cells

Several *in vitro* studies have demonstrated that LCN2 protects against cellular stress and exposure to H_2O_2 (33–37). Other studies have reported that oxidative stress plays a major role in degenerative retinal diseases such as RP and AMD (38–41). To investigate the effects of LCN2 on H_2O_2-induced oxidative stress in RPE cells, 1 ng/ml of LCN2 was incubated with hiPS-RPE cells under oxidative stress conditions (Fig. 8A). Incubation with 100 μM of H_2O_2 for 24 h in the absence of LCN2 resulted in reduced cell viability to 49.51±11.59%, indicating that about half the cell population died (Fig. 8A). When 1 ng/ml of LCN2 was added to these incubation conditions, protective effects of LCN2 against H_2O_2-induced cell death were observed. LCN2 supplementation maintained cell viability nearly to the control level at 87.62±12.74%. With increasing doses of recombinant LCN2, increased expression of antioxidant enzymes *HMOX1* and *SOD2* in hiPS-RPE cells was observed (Fig. 8B, 8C), suggesting that an upregulation of HMOX1and SOD2 is an adaptive mechanism to protect cells from oxidative damage. HMOX1 and SOD2 are known to act as the first line antioxidant enzyme defense system against ROS and particularly superoxide anion radicals (40).

LCN2 has anti-apoptotic effects in the RPE

Retinal inflammation has detrimental effects on cell viability (27, 42–44). To examine whether LCN2 could protect RPE cells from inflammation-associated cell death, hiPS-RPE cells were incubated with 1 μg/ml of LPS for 24 h in the absence and presence of LCN2. Caspase 3/7 expression was measured to assess cell apoptosis. Increased numbers of apoptotic cells were detected in LPS treated cells in the absence of LCN2. When hiPS-RPE cells were pretreated with 10 or 100 ng/ml of LCN2 for 24 h before incubation with 1 μg/ml of LPS, a reduction in the number of apoptotic cells was observed as compared with the LPS only-treated group (Fig. 9). Anti-immune reactions of LCN2 were observed in human RPE-derived cells when these cells were cultured with LCN2 (supplemental Fig. 2). These results suggest that LCN2 provides protection from inflammation-associated cell death.

Expression of LCN2 receptor in RPE cells

LCN2 is known to modulate cell homeostasis by its interaction with specific cell-surface receptors, namely murine 24p3r (45–47) and SLC22A17 (the solute carrier family 22 member 17) which belongs to the major cation transporter family in humans. To explore the possible involvement of a receptor mediated effect, expression of LCN2 receptor in RPE cells was examined. Expression of *SLC22A17* was detected in human RPE cells including hiPS-RPE, ARPE19 (a human RPE derived cell line) and primary human RPE cells (Fig. 10A). When *Abca4*$^{-/-}$*Rdh8*$^{-/-}$ mice were exposed to light exposure at 10,000 lux for 30 min, qRT-PCR revealed that *24p3r* expression increased in the RPE cells after light exposure (Fig. 10B), suggesting the possible involvement of RPE-LCN2 interaction during retinal degeneration pathogenesis.

Patients with Stargardt disease, RP and AMD have higher LCN2 plasma levels

To investigate roles of LCN2 in human retinal degenerative diseases, LCN2 plasma levels in patients with Stargardt disease, RP and AMD were measured and compared to age-matched control individuals without any retinal diseases (supplemental Fig. 3). Determined LCN2 plasma concentrations were as follows: 45.13 ± 5.37 ng/ml in Stargardt disease (n=11), 44.78 ±31.73 ng/ml in RP (n=117), 48.41 ± 28.52 ng/ml in AMD (n=57) and 17.04 ± 11.9 ng/ml in controls (n=77). Patients with these retinal degenerative diseases exhibited higher plasma levels of LCN2 as compared with control individuals, suggesting roles of LCN2 in human diseases.

Overexpression of LCN2 prevented LPS-induced cell death in RPE cells

Lastly, protective effects of LCN2 from RPE cell death were examined. ARPE19 cells were overexpressed *LCN2*, and then these cells were cultured with 1 μg/ml of LPS for 24 h to induce inflammation-associated cell death. *LCN2*-transfected cells demonstrated better cell viability as compared with control vector transfected cells (Figure 11A). Transfection of *LCN2* successfully increased *LCN2* levels in ARPE19 cells (Figure 11B).

Discussion

Millions of people around the world suffer from retinal degenerative diseases such as inherited retinal dystrophies and AMD, with major debilitating impact on daily life. Apoptosis and inflammation play important roles in the pathogenesis of these diseases. Previous studies have demonstrated that retinal inflammation contributes to retinal degeneration (19) and that increased expression of an acute stress protein LCN2 is observed in $Abca4^{-/-}Rdh8^{-/-}$ mice after light exposure (3). In the present study, *Lcn2* expression was increased in the brain as well as in the eye 1 day after light exposure in $Abca4^{-/-}Rdh8^{-/-}$ mice with LCN2 production observed in RPE and retinal microglial cells. We also compared $Lcn2^{-/-}Abca4^{-/-}Rdh8^{-/-}$ mice with $Abca4^{-/-}Rdh8^{-/-}$ mice after exposure to light and found that deficiency of *Lcn2* resulted in more severe retinal damage and increased expression of inflammatory cytokines including *Ccl8, Ccl2 and Cxcl10. Lcn2* loss also resulted in increased expression of one of the receptors of CCL3, namely *Ccr5*. Our previous work has shown that CCL2 and CCL3 have distinct roles in the pathogenesis of retinal degeneration in $Abca4^{-/-}Rdh8^{-/-}$ mice (27). In other published studies, mice lacking *Lcn2* exhibited impaired migration of astrocytes to injury sites with decreased *Cxcl10* expression (48). This observation suggests that LCN2 protein, secreted under inflammatory conditions, could amplify neuroinflammation by inducing neural immune cells to secrete chemokines such as CXCL10 for recruiting additional inflammatory cells. Unexpectedly, we observed in the present study an increased number of activated microglial cells in light exposed $Lcn2^{-/-}Abca4^{-/-}Rdh8^{-/-}$ mice as compared to $Abca4^{-/-}Rdh8^{-/-}$ mice, with $Lcn2^{-/-}Abca4^{-/-}Rdh8^{-/-}$ mice exhibiting increased *Cxcl10* expression. Activation of microglial cells in response to chemokines, including CCL2 produced from the RPE, is a hallmark of inflammation in retinal degeneration (27). Activated microglial cells in the subretinal space display increased production of pro-inflammatory and chemotactic cytokines (27).

The current study demonstrated protective roles of LCN2 in retinal degeneration as other reported studies, however there are conflicting observations (49–56) and both pro- and anti-inflammatory properties of this glycoprotein have been reported. LCN2 expression can be induced by several cytokines and growth factors, including IL-6, IL-1β, IL-10, IL-17, tumor necrosis factor (TNF) and tumor growth factor (TGF) (57–62). Such LCN2 induction is dependent on the activation of NF-kB transcriptional activity, which is suggested as a positive regulator of LCN2 expression itself (28). Another report suggested that LCN2 plays a role as an anti-inflammatory regulator of macrophage polarization and NF-kB/STAT3 pathway activation (52). This study demonstrated that LPS stimulation elicited an increase in the activation of NF-kB, c-Jun, and STAT3 signaling pathways in *Lcn2*$^{-/-}$ bone marrow-derived macrophages (BMDMs). Pretreatment with recombinant LCN2 attenuated LPS-stimulated degradation of Ik-Ba and STAT3 phosphorylation as well as LPS-induced gene expression of IL6 and iNOS in *Lcn2*$^{-/-}$ BMDMs. Here, we investigated the regulation of LCN2 in RPE cells. Pretreatment of hiPS-RPE cells with LCN2 before exposing to LPS resulted in a significant decrease in nuclear translocation of NF-kB p65, suggesting a negative feedback loop involving LCN2. We also found LCN2 murine receptor 24p3r expression in RPE cells increased in a similar fashion as LCN2 after light exposure in *Abca4*$^{-/-}$*Rdh8*$^{-/-}$ mice, implicating LCN2 receptor and agonist interactions in RPE cells. Though LCN2 signaling pathways are not fully elucidated, it is noteworthy that LCN2 promoter region contains the binding sites of several transcription factors such as STAT1, STAT3, CREB, and C/EBPβ and NF-κB (28).

The antioxidant function of LCN2 has been well characterized (33, 35, 63) and the protein shown to be cytoprotective against oxidative stress (37, 64, 65). LCN2 protects against cellular stress from exposure to H_2O_2 and that overexpression of LCN2 allows cells to better tolerate oxidative stress conditions (6). Our current results show that expression of LCN2 in hiPS-RPE cells suppresses H_2O_2-induced cell death and prolongs cell survival. We found the transcripts levels of the key oxidative stress-catalyzing enzymes HMOX1 and SOD2 increased with increasing LCN2 concentrations, supporting an antioxidant role for LCN2 in RPE cells. HMOX1 not only regulates the cellular content of the pro-oxidant heme, but also produces catabolites with regulatory and protective functions (66). SODs mRNA levels increase following a wide range of mechanical, chemical, and biological stimuli that increase reactive oxygen species (ROS), such as UVB and X-irradiation, ozone, and LPS (67). Increased gene expression of SODs and heme oxygenases are adaptive cellular defense mechanisms against oxidative stress. In our animal study, loss of *Lcn2* in mice resulted in more severe retinal degeneration after light exposure. In the retina LCN2 may serve to protect from a broad array of ROS produced by light exposure (68–70), including ROS generated in the visual cycle from the conversion of 11-*cis*-retinal to all-*trans*-retinal (19, 68).

LCN2 in biological fluids under healthy conditions is in low concentration, but the protein can be upregulated by inflammation and becomes detectable at various stages in several diseases (71–74). We found LCN2 plasma levels elevated over 2-fold in patients with Stargardt disease, RP and AMD compared with healthy controls. In this study, LCN2 expression was observed in the retinal pigmented epithelium (RPE) and in the inner retina. An earlier report demonstrated that RPE is a main source of secreted LCN2 in the eye (14).

Because breakdown of the blood retinal barrier (BRB) can be observed during the process of retinal degeneration (19), such comprised BRB might contribute to leakage of LCN2 produced in the eye and to increased levels of LCN2 in plasma of patients. Activated immune cells, which produce LCN2, could migrate into the blood vessels and produce LCN2 into the blood. This result not only implies potentially important roles for circulating LCN2 in the pathogenesis of retinal degenerative diseases, but also the possibility that LCN2 could serve as a biomarker of early disease onset and progression (75).

In conclusion, this study provides evidence that LCN2 may serve to protect the retina from inflammation induced degeneration through regulation of cytokine and chemokine production, and by preserving cell viability and attenuating apoptosis through regulation of anti-oxidant enzymes. LCN2, secreted mainly from RPE cells in the retina, could be a critical mediator in retinal inflammation and degeneration processes.

Supplementary Material

Refer to Web version on PubMed Central for supplementary material.

Acknowledgments

Grant Information: This work was supported by funding from the NIH (EY022658 and EY11373), Research to Prevent Blindness Foundation, and Ohio Lions Eye Research Foundation.

We thank Catherine Dollar and Scott Howell (Visual Science Research Center, Case Western Reserve Univ.), Tatiana Reidel (Department of Ophthalmology and Visual Sciences, University Hospital of Cleveland), Drs. Yuki Arai, Akiko Yoshida and Kanako Kawai (RIKEN) for their technical assistance and comments.

Abbreviations used in the article

ABCA4	ATP binding cassette subfamily A member 4
AMD	age-related macular degeneration
GFAP	glial fibrillary acidic protein
hiPS-RPE	human induced pluripotent stem cell derived retinal pigmented epithelium
HMOX1	heme oxygenase 1
LCN2	lipocalin 2
LPS	lipopolysaccharide
RP	retinitis pigmentosa
RPE	retinal pigmented epithelium
ONL	outer nuclear layer
POS	photoreceptor outer segments
RDH8	retinol dehydrogenase 8

SLO	scanning laser ophthalmoscopy
SOD2	superoxide dismutase 2
WT	wild type

References

1. Wunderlich KA, Leveillard T, Penkowa M, Zrenner E, Perez MT. Altered expression of metallothionein-I and -II and their receptor megalin in inherited photoreceptor degeneration. Invest Ophthalmol Vis Sci. 2010; 51:4809–4820. [PubMed: 20357188]
2. Ambati J, Atkinson JP, Gelfand BD. Immunology of age-related macular degeneration. Nat Rev Immunol. 2013; 13:438–451. [PubMed: 23702979]
3. Parmar T V, Parmar M, Arai E, Sahu B, Perusek L, Maeda A. Acute Stress Responses Are Early Molecular Events of Retinal Degeneration in Abca4−/−Rdh8−/− Mice After Light Exposure. Invest Ophthalmol Vis Sci. 2016; 57:3257–3267. [PubMed: 27315541]
4. Saha P, Chassaing B, Yeoh BS, Viennois E, Xiao X, Kennett MJ, Singh V, Vijay-Kumar M. Ectopic Expression of Innate Immune Protein, Lipocalin-2, in Lactococcus lactis Protects Against Gut and Environmental Stressors. Inflamm Bowel Dis. 2017; 23:1120–1132. [PubMed: 28445245]
5. Kang SS, Ren Y, Liu CC, Kurti A, Baker KE, Bu G, Asmann Y, Fryer JD. Lipocalin-2 protects the brain during inflammatory conditions. Mol Psychiatry. 2017
6. Srinivasan G, Aitken JD, Zhang B, Carvalho FA, Chassaing B, Shashidharamurthy R, Borregaard N, Jones DP, Gewirtz AT, Vijay-Kumar M. Lipocalin 2 deficiency dysregulates iron homeostasis and exacerbates endotoxin-induced sepsis. J Immunol. 2012; 189:1911–1919. [PubMed: 22786765]
7. Borkham-Kamphorst E, van de Leur E, Zimmermann HW, Karlmark KR, Tihaa L, Haas U, Tacke F, Berger T, Mak TW, Weiskirchen R. Protective effects of lipocalin-2 (LCN2) in acute liver injury suggest a novel function in liver homeostasis. Biochim Biophys Acta. 2013; 1832:660–673. [PubMed: 23376114]
8. Asimakopoulou A, Fulop A, Borkham-Kamphorst E, de Leur EV, Gassler N, Berger T, Beine B, Meyer HE, Mak TW, Hopf C, Henkel C, Weiskirchen R. Altered mitochondrial and peroxisomal integrity in lipocalin-2-deficient mice with hepatic steatosis. Biochim Biophys Acta. 2017; 1863:2093–2110. [PubMed: 28396286]
9. Asimakopoulou A, Borkham-Kamphorst E, de Leur EV, Weiskirchen R. Data on Lipocalin 2 and phosphatidylinositol 3-kinase signaling in a methionine- and choline-deficient model of non-alcoholic steatohepatitis. Data Brief. 2017; 13:644–649. [PubMed: 28725667]
10. Mori K, Lee HT, Rapoport D, Drexler IR, Foster K, Yang J, Schmidt-Ott KM, Chen X, Li JY, Weiss S, Mishra J, Cheema FH, Markowitz G, Suganami T, Sawai K, Mukoyama M, Kunis C, D'Agati V, Devarajan P, Barasch J. Endocytic delivery of lipocalin-siderophore-iron complex rescues the kidney from ischemia-reperfusion injury. J Clin Invest. 2005; 115:610–621. [PubMed: 15711640]
11. Abcouwer SF, Lin CM, Shanmugam S, Muthusamy A, Barber AJ, Antonetti DA. Minocycline prevents retinal inflammation and vascular permeability following ischemia-reperfusion injury. J Neuroinflammation. 2013; 10:149. [PubMed: 24325836]
12. Swiderski RE, Nishimura DY, Mullins RF, Olvera MA, Ross JL, Huang J, Stone EM, Sheffield VC. Gene expression analysis of photoreceptor cell loss in bbs4-knockout mice reveals an early stress gene response and photoreceptor cell damage. Invest Ophthalmol Vis Sci. 2007; 48:3329–3340. [PubMed: 17591906]
13. Chun BY, Kim JH, Nam Y, Huh MI, Han S, Suk K. Pathological Involvement of Astrocyte-Derived Lipocalin-2 in the Demyelinating Optic Neuritis. Invest Ophthalmol Vis Sci. 2015; 56:3691–3698. [PubMed: 26047170]
14. Valapala M, Edwards M, Hose S, Grebe R, Bhutto IA, Cano M, Berger T, Mak TW, Wawrousek E, Handa JT, Lutty GA, Samuel Zigler J Jr, Sinha D. Increased Lipocalin-2 in the retinal pigment epithelium of Cryba1 cKO mice is associated with a chronic inflammatory response. Aging Cell. 2014; 13:1091–1094. [PubMed: 25257511]

15. Ghosh S, Shang P, Yazdankhah M, Bhutto I, Hose S, Montezuma SR, Luo T, Chattopadhyay S, Qian J, Lutty GA, Ferrington DA, Zigler JS Jr, Sinha D. Activating the AKT2-nuclear factor-kappaB-lipocalin-2 axis elicits an inflammatory response in age-related macular degeneration. J Pathol. 2017; 241:583–588. [PubMed: 28026019]
16. Maeda A, Maeda T, Golczak M, Palczewski K. Retinopathy in mice induced by disrupted all-trans-retinal clearance. J Biol Chem. 2008; 283:26684–26693. [PubMed: 18658157]
17. Haeseleer F, Jang GF, Imanishi Y, Driessen C, Matsumura M, Nelson PS, Palczewski K. Dual-substrate specificity short chain retinol dehydrogenases from the vertebrate retina. J Biol Chem. 2002; 277:45537–45546. [PubMed: 12226107]
18. Maeda A, Maeda T, Imanishi Y, Kuksa V, Alekseev A, Bronson JD, Zhang H, Zhu L, Sun W, Saperstein DA, Rieke F, Baehr W, Palczewski K. Role of photoreceptor-specific retinol dehydrogenase in the retinoid cycle in vivo. J Biol Chem. 2005; 280:18822–18832. [PubMed: 15755727]
19. Kohno H, Chen Y, Kevany BM, Pearlman E, Miyagi M, Maeda T, Palczewski K, Maeda A. Photoreceptor proteins initiate microglial activation via Toll-like receptor 4 in retinal degeneration mediated by all-trans-retinal. J Biol Chem. 2013; 288:15326–15341. [PubMed: 23572532]
20. Perusek L, Sahu B, Parmar T, Maeno H, Arai E, Le YZ, Subauste CS, Chen Y, Palczewski K, Maeda A. Di-retinoid-pyridinium-ethanolamine (A2E) Accumulation and the Maintenance of the Visual Cycle Are Independent of Atg7-mediated Autophagy in the Retinal Pigmented Epithelium. J Biol Chem. 2015; 290:29035–29044. [PubMed: 26468292]
21. Osakada F, Ikeda H, Sasai Y, Takahashi M. Stepwise differentiation of pluripotent stem cells into retinal cells. Nat Protoc. 2009; 4:811–824. [PubMed: 19444239]
22. Kokkinaki M, Sahibzada N, Golestaneh N. Human induced pluripotent stem-derived retinal pigment epithelium (RPE) cells exhibit ion transport, membrane potential, polarized vascular endothelial growth factor secretion, and gene expression pattern similar to native RPE. Stem Cells. 2011; 29:825–835. [PubMed: 21480547]
23. Maeda T, Lee MJ, Palczewska G, Marsili S, Tesar PJ, Palczewski K, Takahashi M, Maeda A. Retinal pigmented epithelial cells obtained from human induced pluripotent stem cells possess functional visual cycle enzymes in vitro and in vivo. J Biol Chem. 2013; 288:34484–34493. [PubMed: 24129572]
24. Carr AJ, Vugler AA, Hikita ST, Lawrence JM, Gias C, Chen LL, Buchholz DE, Ahmado A, Semo M, Smart MJ, Hasan S, da Cruz L, Johnson LV, Clegg DO, Coffey PJ. Protective effects of human iPS-derived retinal pigment epithelium cell transplantation in the retinal dystrophic rat. PLoS One. 2009; 4:e8152. [PubMed: 19997644]
25. Buchholz DE, Hikita ST, Rowland TJ, Friedrich AM, Hinman CR, Johnson LV, Clegg DO. Derivation of functional retinal pigmented epithelium from induced pluripotent stem cells. Stem Cells. 2009; 27:2427–2434. [PubMed: 19658190]
26. Gu J, Pauer GJ, Yue X, Narendra U, Sturgill GM, Bena J, Gu X, Peachey NS, Salomon RG, Hagstrom SA, Crabb JW. G. Clinical, and A.M.D.S.G. Proteomic. Assessing susceptibility to age-related macular degeneration with proteomic and genomic biomarkers. Mol Cell Proteomics. 2009; 8:1338–1349. [PubMed: 19202148]
27. Kohno H, Maeda T, Perusek L, Pearlman E, Maeda A. CCL3 production by microglial cells modulates disease severity in murine models of retinal degeneration. J Immunol. 2014; 192:3816–3827. [PubMed: 24639355]
28. Zhao P, Stephens JM. STAT1, NF-kappaB and ERKs play a role in the induction of lipocalin-2 expression in adipocytes. Mol Metab. 2013; 2:161–170. [PubMed: 24049731]
29. Lawrence T. The nuclear factor NF-kappaB pathway in inflammation. Cold Spring Harb Perspect Biol. 2009; 1:a001651. [PubMed: 20457564]
30. Kamoshita M, Ozawa Y, Kubota S, Miyake S, Tsuda C, Nagai N, Yuki K, Shimmura S, Umezawa K, Tsubota K. AMPK-NF-kappaB axis in the photoreceptor disorder during retinal inflammation. PLoS One. 2014; 9:e103013. [PubMed: 25048039]
31. Gasparini C, Feldmann M. NF-kappaB as a target for modulating inflammatory responses. Curr Pharm Des. 2012; 18:5735–5745. [PubMed: 22726116]

32. Zeng HY, Tso MO, Lai S, Lai H. Activation of nuclear factor-kappaB during retinal degeneration in rd mice. Mol Vis. 2008; 14:1075–1080. [PubMed: 18552981]
33. Roudkenar MH, Kuwahara Y, Baba T, Roushandeh AM, Ebishima S, Abe S, Ohkubo Y, Fukumoto M. Oxidative stress induced lipocalin 2 gene expression: addressing its expression under the harmful conditions. J Radiat Res. 2007; 48:39–44. [PubMed: 17229997]
34. Lechner M, Wojnar P, Redl B. Human tear lipocalin acts as an oxidative-stress-induced scavenger of potentially harmful lipid peroxidation products in a cell culture system. Biochem J. 2001; 356:129–135. [PubMed: 11336644]
35. Roudkenar MH, Halabian R, Bahmani P, Roushandeh AM, Kuwahara Y, Fukumoto M. Neutrophil gelatinase-associated lipocalin: a new antioxidant that exerts its cytoprotective effect independent on Heme Oxygenase-1. Free Radic Res. 2011; 45:810–819. [PubMed: 21545264]
36. Roudkenar MH, Halabian R, Oodi A, Roushandeh AM, Yaghmai P, Najar MR, Amirizadeh N, Shokrgozar MA. Upregulation of neutrophil gelatinase-associated lipocalin, NGAL/Lcn2, in beta-thalassemia patients. Arch Med Res. 2008; 39:402–407. [PubMed: 18375251]
37. Roudkenar MH, Halabian R, Ghasemipour Z, Roushandeh AM, Rouhbakhsh M, Nekogoftar M, Kuwahara Y, Fukumoto M, Shokrgozar MA. Neutrophil gelatinase-associated lipocalin acts as a protective factor against H(2)O(2) toxicity. Arch Med Res. 2008; 39:560–566. [PubMed: 18662586]
38. Chiras D, Kitsos G, Petersen MB, Skalidakis I, Kroupis C. Oxidative stress in dry age-related macular degeneration and exfoliation syndrome. Crit Rev Clin Lab Sci. 2015; 52:12–27. [PubMed: 25319011]
39. Datta S, Cano M, Ebrahimi K, Wang L, Handa JT. The impact of oxidative stress and inflammation on RPE degeneration in non-neovascular AMD. Prog Retin Eye Res. 2017; 60:201–218. [PubMed: 28336424]
40. Ugurlu N, Asik MD, Yulek F, Neselioglu S, Cagil N. Oxidative stress and anti-oxidative defence in patients with age-related macular degeneration. Curr Eye Res. 2013; 38:497–502. [PubMed: 23432778]
41. Yildirim Z, Ucgun NI, Yildirim F. The role of oxidative stress and antioxidants in the pathogenesis of age-related macular degeneration. Clinics (Sao Paulo). 2011; 66:743–746. [PubMed: 21789374]
42. Rutar M, Natoli R, Chia RX, Valter K, Provis JM. Chemokine-mediated inflammation in the degenerating retina is coordinated by Muller cells, activated microglia, and retinal pigment epithelium. J Neuroinflammation. 2015; 12:8. [PubMed: 25595590]
43. Juel HB, Faber C, Svendsen SG, Vallejo AN, Nissen MH. Inflammatory cytokines protect retinal pigment epithelial cells from oxidative stress-induced death. PLoS One. 2013; 8:e64619. [PubMed: 23705001]
44. Ardeljan CP, Ardeljan D, Abu-Asab M, Chan CC. Inflammation and Cell Death in Age-Related Macular Degeneration: An Immunopathological and Ultrastructural Model. J Clin Med. 2014; 3:1542–1560. [PubMed: 25580276]
45. Devireddy LR, Gazin C, Zhu X, Green MR. A cell-surface receptor for lipocalin 24p3 selectively mediates apoptosis and iron uptake. Cell. 2005; 123:1293–1305. [PubMed: 16377569]
46. Hvidberg V, Jacobsen C, Strong RK, Cowland JB, Moestrup SK, Borregaard N. The endocytic receptor megalin binds the iron transporting neutrophil-gelatinase-associated lipocalin with high affinity and mediates its cellular uptake. FEBS Lett. 2005; 579:773–777. [PubMed: 15670845]
47. Langelueddecke C, Roussa E, Fenton RA, Thevenod F. Expression and function of the lipocalin-2 (24p3/NGAL) receptor in rodent and human intestinal epithelia. PLoS One. 2013; 8:e71586. [PubMed: 23940770]
48. Lee S, Kim JH, Kim JH, Seo JW, Han HS, Lee WH, Mori K, Nakao K, Barasch J, Suk K. Lipocalin-2 Is a chemokine inducer in the central nervous system: role of chemokine ligand 10 (CXCL10) in lipocalin-2-induced cell migration. J Biol Chem. 2011; 286:43855–43870. [PubMed: 22030398]
49. Aigner F, Maier HT, Schwelberger HG, Wallnofer EA, Amberger A, Obrist P, Berger T, Mak TW, Maglione M, Margreiter R, Schneeberger S, Troppmair J. Lipocalin-2 regulates the inflammatory response during ischemia and reperfusion of the transplanted heart. Am J Transplant. 2007; 7:779–788. [PubMed: 17391123]

50. Berard JL, Zarruk JG, Arbour N, Prat A, Yong VW, Jacques FH, Akira S, David S. Lipocalin 2 is a novel immune mediator of experimental autoimmune encephalomyelitis pathogenesis and is modulated in multiple sclerosis. Glia. 2012; 60:1145–1159. [PubMed: 22499213]
51. Chakraborty S, Kaur S, Guha S, Batra SK. The multifaceted roles of neutrophil gelatinase associated lipocalin (NGAL) in inflammation and cancer. Biochim Biophys Acta. 2012; 1826:129–169. [PubMed: 22513004]
52. Guo H, Jin D, Chen X. Lipocalin 2 is a regulator of macrophage polarization and NF-kappaB/STAT3 pathway activation. Mol Endocrinol. 2014; 28:1616–1628. [PubMed: 25127375]
53. Nam Y, Kim JH, Seo M, Kim JH, Jin M, Jeon S, Seo JW, Lee WH, Bing SJ, Jee Y, Lee WK, Park DH, Kook H, Suk K. Lipocalin-2 protein deficiency ameliorates experimental autoimmune encephalomyelitis: the pathogenic role of lipocalin-2 in the central nervous system and peripheral lymphoid tissues. J Biol Chem. 2014; 289:16773–16789. [PubMed: 24808182]
54. Shashidharamurthy R, Machiah D, Aitken JD, Putty K, Srinivasan G, Chassaing B, Parkos CA, Selvaraj P, Vijay-Kumar M. Differential role of lipocalin 2 during immune complex-mediated acute and chronic inflammation in mice. Arthritis Rheum. 2013; 65:1064–1073. [PubMed: 23280250]
55. Wang Y, Lam KS, Kraegen EW, Sweeney G, Zhang J, Tso AW, Chow WS, Wat NM, Xu JY, Hoo RL, Xu A. Lipocalin-2 is an inflammatory marker closely associated with obesity, insulin resistance, and hyperglycemia in humans. Clin Chem. 2007; 53:34–41. [PubMed: 17040956]
56. Zhang Y, Foncea R, Deis JA, Guo H, Bernlohr DA, Chen X. Lipocalin 2 expression and secretion is highly regulated by metabolic stress, cytokines, and nutrients in adipocytes. PLoS One. 2014; 9:e96997. [PubMed: 24818605]
57. Borkham-Kamphorst E, Drews F, Weiskirchen R. Induction of lipocalin-2 expression in acute and chronic experimental liver injury moderated by pro-inflammatory cytokines interleukin-1beta through nuclear factor-kappaB activation. Liver Int. 2011; 31:656–665. [PubMed: 21457438]
58. Bu DX, Hemdahl AL, Gabrielsen A, Fuxe J, Zhu C, Eriksson P, Yan ZQ. Induction of neutrophil gelatinase-associated lipocalin in vascular injury via activation of nuclear factor-kappaB. Am J Pathol. 2006; 169:2245–2253. [PubMed: 17148685]
59. Hamzic N, Blomqvist A, Nilsberth C. Immune-induced expression of lipocalin-2 in brain endothelial cells: relationship with interleukin-6, cyclooxygenase-2 and the febrile response. J Neuroendocrinol. 2013; 25:271–280. [PubMed: 23046379]
60. Sorensen OE, Cowland JB, Theilgaard-Monch K, Liu L, Ganz T, Borregaard N. Wound healing and expression of antimicrobial peptides/polypeptides in human keratinocytes, a consequence of common growth factors. J Immunol. 2003; 170:5583–5589. [PubMed: 12759437]
61. Vazquez DE, Nino DF, De Maio A, Cauvi DM. Sustained expression of lipocalin-2 during polymicrobial sepsis. Innate Immun. 2015; 21:477–489. [PubMed: 25227123]
62. Xu MJ, Feng D, Wu H, Wang H, Chan Y, Kolls J, Borregaard N, Porse B, Berger T, Mak TW, Cowland JB, Kong X, Gao B. Liver is the major source of elevated serum lipocalin-2 levels after bacterial infection or partial hepatectomy: a critical role for IL-6/STAT3. Hepatology. 2015; 61:692–702. [PubMed: 25234944]
63. Yamada Y, Miyamoto T, Kashima H, Kobara H, Asaka R, Ando H, Higuchi S, Ida K, Shiozawa T. Lipocalin 2 attenuates iron-related oxidative stress and prolongs the survival of ovarian clear cell carcinoma cells by up-regulating the CD44 variant. Free Radic Res. 2016; 50:414–425. [PubMed: 26729415]
64. Halabian R, Tehrani HA, Jahanian-Najafabadi A, Habibi Roudkenar M. Lipocalin-2-mediated upregulation of various antioxidants and growth factors protects bone marrow-derived mesenchymal stem cells against unfavorable microenvironments. Cell Stress Chaperones. 2013; 18:785–800. [PubMed: 23620204]
65. Roudkenar MH, Halabian R, Roushandeh AM, Nourani MR, Masroori N, Ebrahimi M, Nikogoftar M, Rouhbakhsh M, Bahmani P, Najafabadi AJ, Shokrgozar MA. Lipocalin 2 regulation by thermal stresses: protective role of Lcn2/NGAL against cold and heat stresses. Exp Cell Res. 2009; 315:3140–3151. [PubMed: 19732769]
66. Immenschuh S, Ramadori G. Gene regulation of heme oxygenase-1 as a therapeutic target. Biochem Pharmacol. 2000; 60:1121–1128. [PubMed: 11007950]

67. Zelko IN, Mariani TJ, Folz RJ. Superoxide dismutase multigene family: a comparison of the CuZn-SOD (SOD1), Mn-SOD (SOD2), and EC-SOD (SOD3) gene structures, evolution, and expression. Free Radic Biol Med. 2002; 33:337–349. [PubMed: 12126755]

68. Chen Y, Okano K, Maeda T, Chauhan V, Golczak M, Maeda A, Palczewski K. Mechanism of all-trans-retinal toxicity with implications for stargardt disease and age-related macular degeneration. J Biol Chem. 2012; 287:5059–5069. [PubMed: 22184108]

69. Maeda A, Golczak M, Chen Y, Okano K, Kohno H, Shiose S, Ishikawa K, Harte W, Palczewska G, Maeda T, Palczewski K. Primary amines protect against retinal degeneration in mouse models of retinopathies. Nat Chem Biol. 2011; 8:170–178. [PubMed: 22198730]

70. Maeda A, Palczewska G, Golczak M, Kohno H, Dong Z, Maeda T, Palczewski K. Two-photon microscopy reveals early rod photoreceptor cell damage in light-exposed mutant mice. Proc Natl Acad Sci U S A. 2014; 111:E1428–1437. [PubMed: 24706832]

71. Abella V, Scotece M, Conde J, Gomez R, Lois A, Pino J, Gomez-Reino JJ, Lago F, Mobasheri A, Gualillo O. The potential of lipocalin-2/NGAL as biomarker for inflammatory and metabolic diseases. Biomarkers. 2015; 20:565–571. [PubMed: 26671823]

72. Bolignano D, Donato V, Coppolino G, Campo S, Buemi A, Lacquaniti A, Buemi M. Neutrophil gelatinase-associated lipocalin (NGAL) as a marker of kidney damage. Am J Kidney Dis. 2008; 52:595–605. [PubMed: 18725016]

73. Haase-Fielitz A, Haase M, Devarajan P. Neutrophil gelatinase-associated lipocalin as a biomarker of acute kidney injury: a critical evaluation of current status. Ann Clin Biochem. 2014; 51:335–351. [PubMed: 24518531]

74. Mishra J, Ma Q, Prada A, Mitsnefes M, Zahedi K, Yang J, Barasch J, Devarajan P. Identification of neutrophil gelatinase-associated lipocalin as a novel early urinary biomarker for ischemic renal injury. J Am Soc Nephrol. 2003; 14:2534–2543. [PubMed: 14514731]

75. Mishra J, Dent C, Tarabishi R, Mitsnefes MM, Ma Q, Kelly C, Ruff SM, Zahedi K, Shao M, Bean J, Mori K, Barasch J, Devarajan P. Neutrophil gelatinase-associated lipocalin (NGAL) as a biomarker for acute renal injury after cardiac surgery. Lancet. 2005; 365:1231–1238. [PubMed: 15811456]

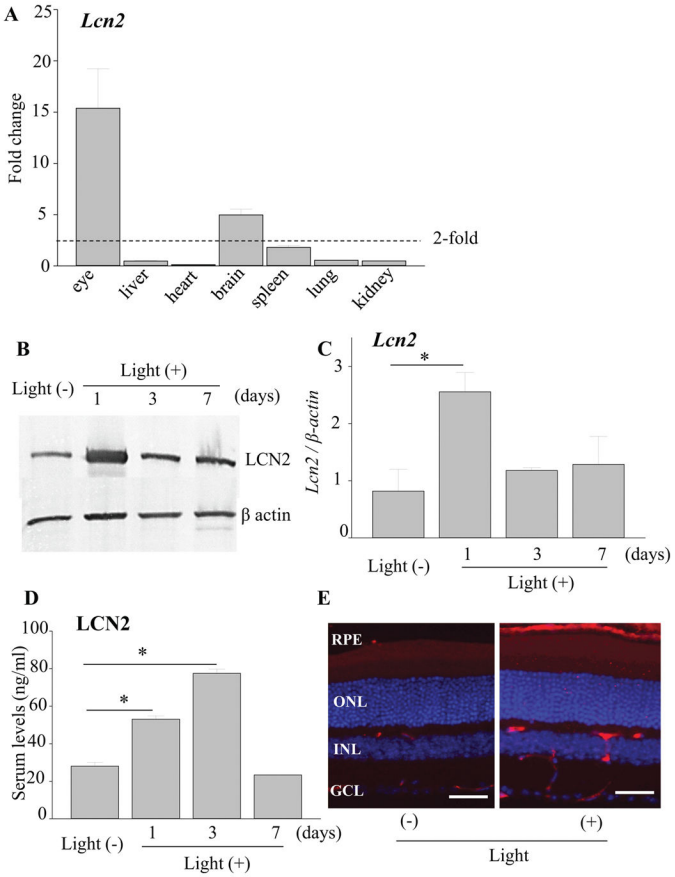

Figure 1. Increased expression of Lcn2 in the retina and brain after light exposure

Abca4$^{-/-}$*Rdh8*$^{-/-}$ mice (1-month-old) were exposed to light at 10,000 lux for 30 min. **A.** Various tissues including the eye, liver, heart, brain, spleen, lung and kidney were collected 24 h after light exposure. RNA levels are presented as fold change over non-light exposed control tissues. **B.** Immunoblot of LCN2 protein in light exposed 1-month-old *Abca4*$^{-/-}$*Rdh8*$^{-/-}$ mice 1, 3, and 7 days after light exposure. **C.** Quantitative analyses of the immunoblot after normalization to β-actin are presented. **D.** Serum was collected from 1-month-old *Abca4*$^{-/-}$*Rdh8*$^{-/-}$ mice at different time points after light exposure. **E.** Immunohistochemistry of LCN2 protein in the retinal sections of 1-month-old *Abca4*$^{-/-}$*Rdh8*$^{-/-}$ mice 24 h after light exposure. Scale bar: 50 μm. RPE, retinal pigmented epithelium; ONL, outer nuclear layer; INL, inner nuclear layer; GCL ganglion cell layer. Error bars indicate S.D. of the means, n=3, *$p < 0.05$.

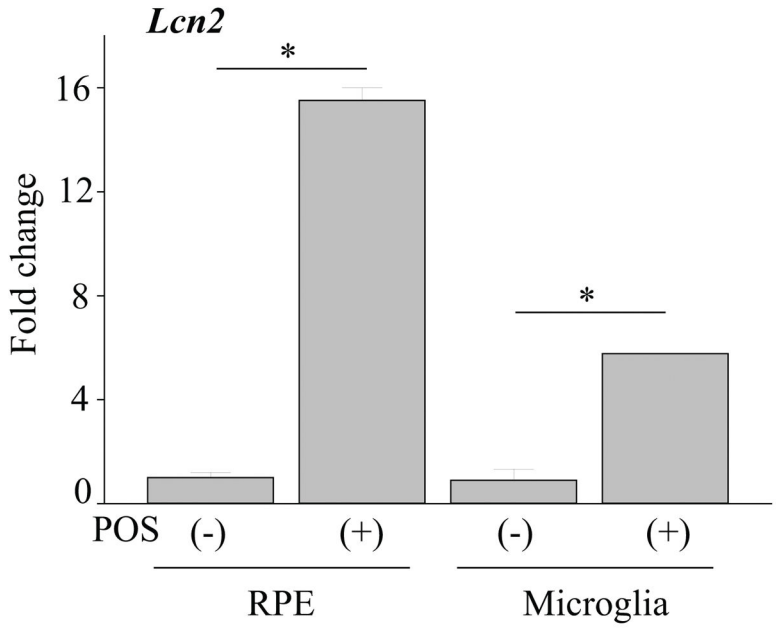

Figure 2. Lcn2 increases in the RPE more than in the microglia

RPE cells and microglia were isolated from 1-month-old *Abca4*$^{-/-}$*Rdh8*$^{-/-}$ mice. Cells were incubated with photoreceptor outer segments (POS, 6 mg/ml) for 24 h. RNA levels of *Lcn2* were measured in both RPE cells and microglia with and without POS. *$p < 0.05$ versus no POS treatment ($n = 6$). Error bars indicate S.D. of the means, *$p < 0.05$.

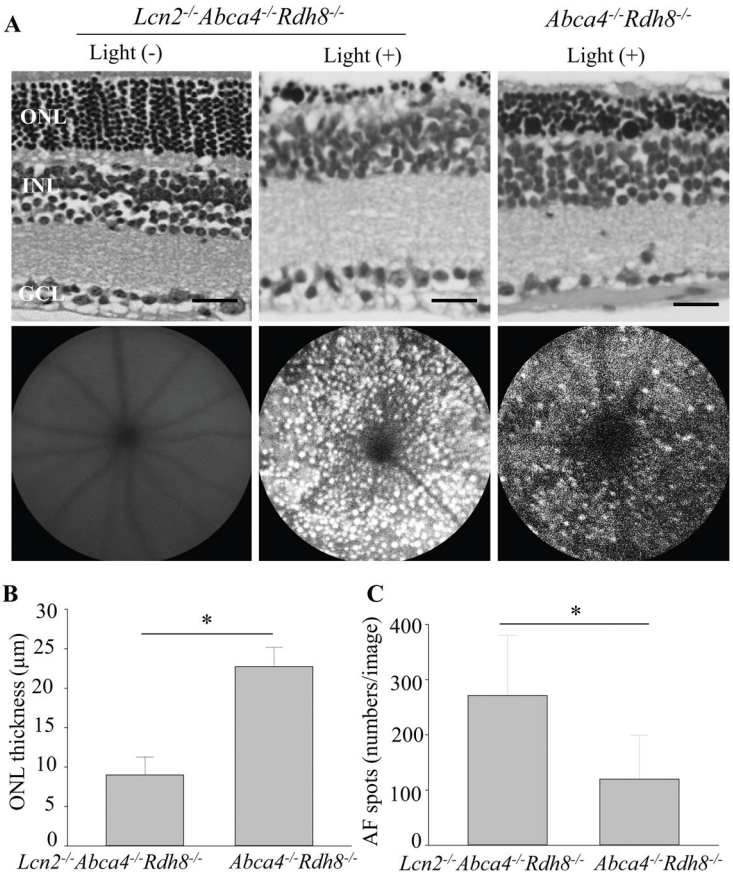

Figure 3. Deficiency of Lcn2 resulted in severe light-induced retinal degeneration in Abca4$^{-/-}$Rdh8$^{-/-}$ mice

A. Representative retinal histology (**upper panel**) and SLO (**lower panel**) of 1-month-old *Lcn2*$^{-/-}$*Abca4*$^{-/-}$*Rdh8*$^{-/-}$ and *Abca4*$^{-/-}$*Rdh8*$^{-/-}$ mice 7 days after light exposure at 10,000 lux for 30 min are shown. Scale bar: 20 μm. **B.** ONL thickness measurements of 1-month-old *Lcn2*$^{-/-}$*Abca4*$^{-/-}$*Rdh8*$^{-/-}$ and *Abca4*$^{-/-}$*Rdh8*$^{-/-}$ mice 7 days after light exposure is presented. **C.** Numbers of autofluorescent (AF) spots detected by SLO in 1-month-old *Lcn2*$^{-/-}$*Abca4*$^{-/-}$*Rdh8*$^{-/-}$ and *Abca4*$^{-/-}$*Rdh8*$^{-/-}$ mice 7 days after light exposure were counted. Error bars indicate S.D. of the means, n=3, *p < 0.05.

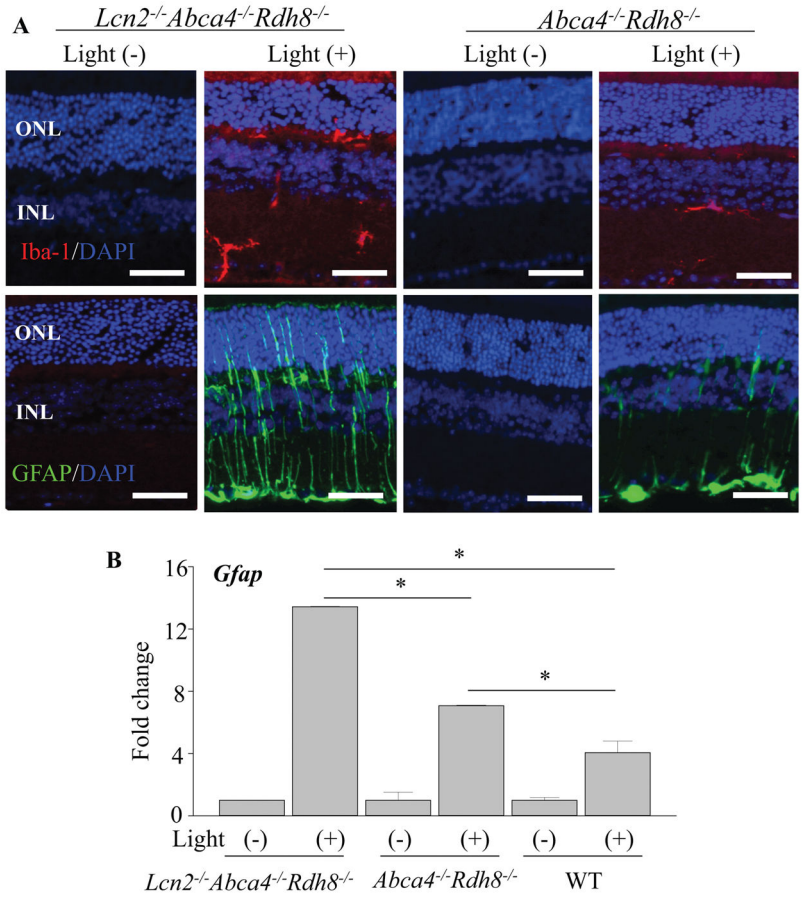

Figure 4. Lcn2$^{-/-}$Abca4$^{-/-}$Rdh8$^{-/-}$ mice showed stronger gliosis than Abca4$^{-/-}$Rdh8$^{-/-}$ mice after light exposure

Lcn2$^{-/-}$*Abca4*$^{-/-}$*Rdh8*$^{-/-}$ and *Abca4*$^{-/-}$*Rdh8*$^{-/-}$ mice at 1 month of age were exposed to light at 10,000 lux for 30 min. **A.** Immunohistochemistry using anti-Iba-1 (in red), a marker of microglia/macrophage in non-light exposed and 24 h after light exposure is presented (**upper panel**). Immunohistochemistry using anti-GFAP (in green), a marker of Müller cells, in non-light exposed and 24 h after light exposure is presented (**lower panel**). Nuclei were stained with DAPI (in blue). **B.** RNA samples were collected from 1-month-old *Lcn2*$^{-/-}$*Abca4*$^{-/-}$*Rdh8*$^{-/-}$, *Abca4*$^{-/-}$*Rdh8*$^{-/-}$ and WT mice. Expression levels of *Gfap* are normalized by *Gapdh* expression and shown by fold change. Error bars indicate S.D. of the means (n = 6). *p < 0.05, Scale bar indicate 50 μm, ONL, outer nuclear layer; INL, inner nuclear layer.

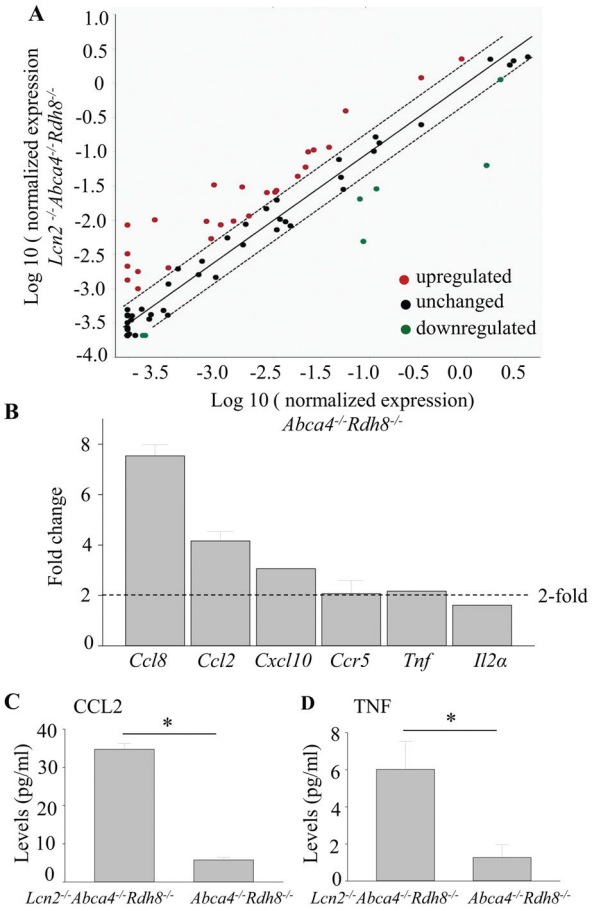

Figure 5. Increased expression of inflammatory response in Lcn2$^{-/-}$Abca4$^{-/-}$Rdh8$^{-/-}$ mice

A. Scatter plot comparing the expression of genes involved in the inflammatory response in *Lcn2*$^{-/-}$*Abca4*$^{-/-}$*Rdh8*$^{-/-}$ and *Abca4*$^{-/-}$*Rdh8*$^{-/-}$ mice 24 h after light exposure at 10,000 lux for 30 min is presented. Each circle represents an individual gene with upregulated genes (in red) and downregulated genes (in green). Genes with no change in regulation (<2-fold in either direction) are within the boundary lines (in black). Genes outside the boundary lines have ≥2-fold altered expression. **B.** RNA samples from whole eyes were collected from 1-month-old *Lcn2*$^{-/-}$*Abca4*$^{-/-}$*Rdh8*$^{-/-}$ and *Abca4*$^{-/-}$*Rdh8*$^{-/-}$ mice 24 h after light exposure. Expression levels of *Ccl8, Ccl2, Cxcl10, Ccr5, Tnf* and *Il2α* are normalized by *Gapdh* expression and shown by fold change. **C, D.** CCL2 and TNF protein levels were measured in 1-month-old *Lcn2*$^{-/-}$*Abca4*$^{-/-}$*Rdh8*$^{-/-}$ and *Abca4*$^{-/-}$*Rdh8*$^{-/-}$ mice 24 h after light exposure. Error bars indicate S.D. of the means, n=6, *p < 0.05.

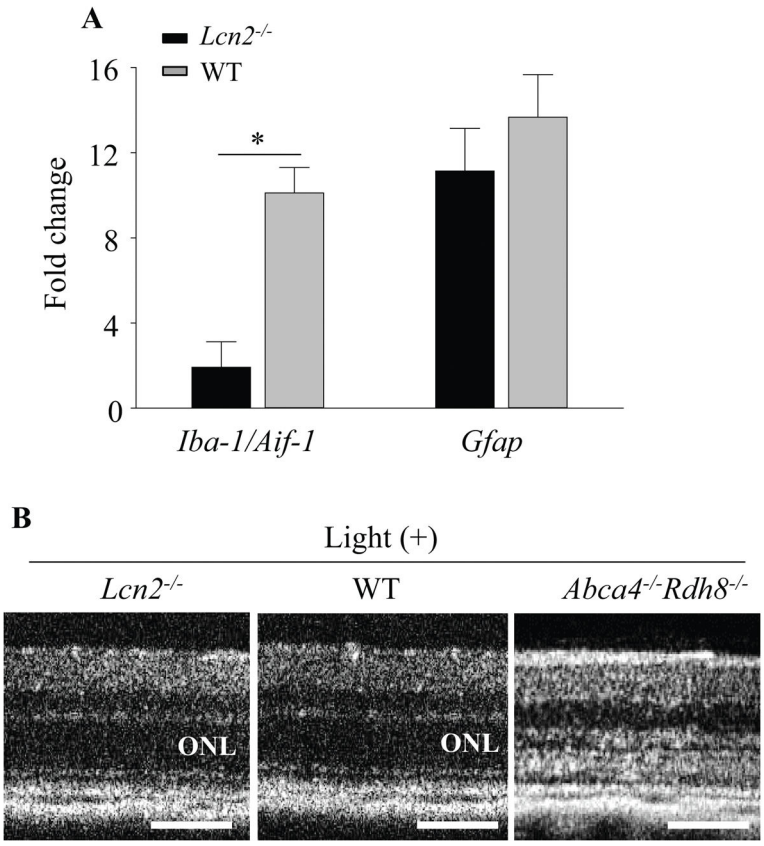

Figure 6. Lcn2$^{-/-}$ mice displayed more preserved retinas with milder inflammation

A. Retinas were isolated from 1-month-old *Lcn2*$^{-/-}$ and wildtype mice 1 day after light exposure at 10,000 lux for 30 min, and expression of *Iba-1/Aif-1* and *Gfap* was examined by qRT-PCR. Error bars indicate S.D. of the means, n=3, *p < 0.05. **B.** Mice were exposed to light and *in vivo* retinal images were obtained using SD-OCT 7 days later. Representative images are presented (n=3). Scale bar indicate 50 μm, ONL, outer nuclear layer.

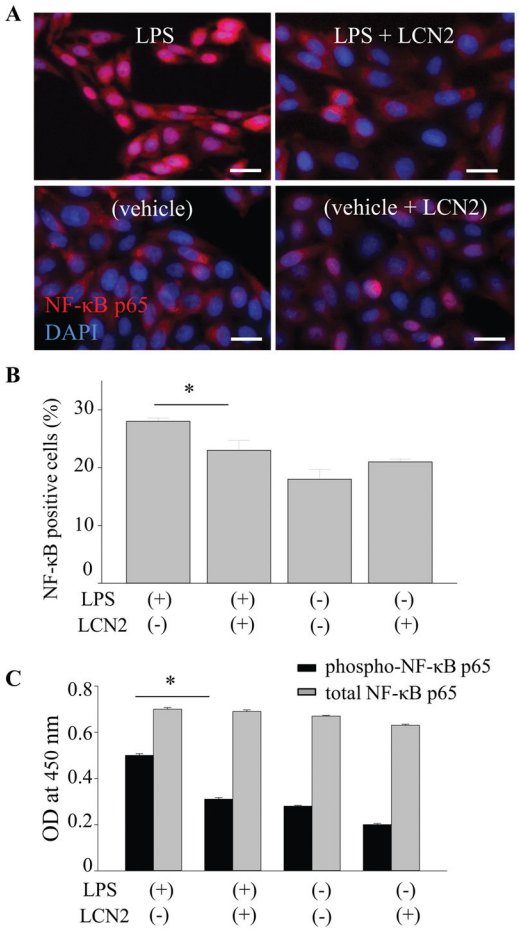

Figure 7. LCN2 attenuated the LPS-stimulated NF-κB activation in RPE cells

A. Human RPE cells differentiated from human induced pluripotent stem (hiPS-RPE) cells were incubated with 1 μg/ml of lipopolysaccharide (LPS) and 1 ng/ml recombinant LCN2 for 24 h. Fluorescence images show anti-NF-κB p65 staining (in red) and nucleus stained by DAPI (in blue). **B.** Quantitative analyses of the ratio of p65-red nuclear fluorescence versus cytoplasmic fluorescence are presented. *$p < 0.05$ versus no LCN2 treatment ($n = 15$). Data are presented as means ± S.D. determined for each experiment independently. Scale bars indicate 20 μm. **C.** hiPS-RPE cells were incubated with 1 μg/ml of LPS and 1 ng/ml recombinant LCN2 for 24 h, and then levels of phosphorylated NF-κB p65 and total NF-κB p65 were quantified using ELISA. *$p < 0.05$ versus no LCN2 treatment ($n = 6$). Data are presented as means ± S.D.

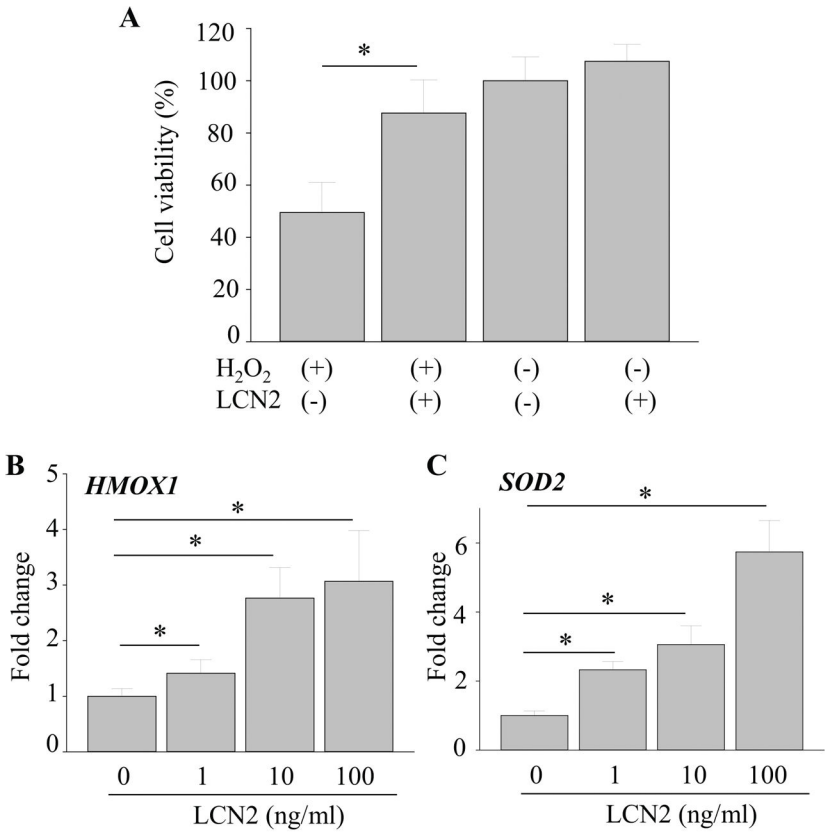

Figure 8. LCN2 protected against oxidative stress by increasing the expression of antioxidant enzymes HMOX1 and SOD2 in hiPS-RPE cells

A. Human RPE cells differentiated from induced pluripotent stem cells (hiPS-RPE) from healthy volunteers was incubated with 1 μg/ml of lipopolysaccharide (LPS) and 1 ng/ml of recombinant LCN2 for 24 h. Cell viability was assessed using WST-1 assay. **B.** RNA was extracted from the cells after 24 h and expression levels of *HMOX1* and *SOD2* were measured. Error bars indicate S.D. of the means, n=15, *p < 0.05.

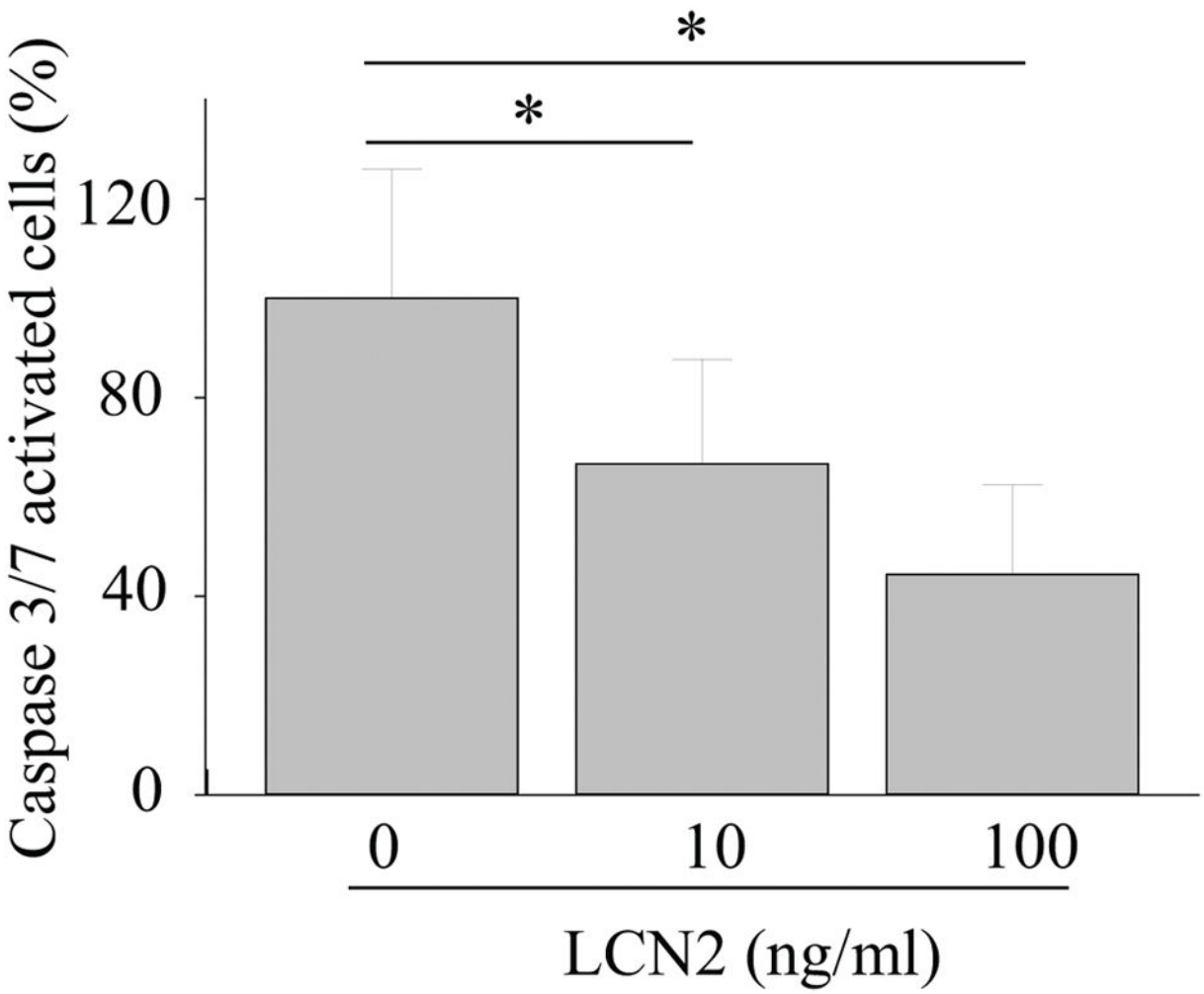

Figure 9. LCN2 displayed anti-apoptotic effects in the RPE

Human RPE cells differentiated from induced pluripotent stem cells (hiPS-RPE) from healthy volunteers was incubated with 1 μg/ml of lipopolysaccharide (LPS) and indicated concentration of recombinant LCN2 for 24 h. Active caspase-3/7 was observed using fluorescence microscopy. Quantitative analyses of the percentage of apoptotic cells were performed from three independent experiments. *$p < 0.05$.

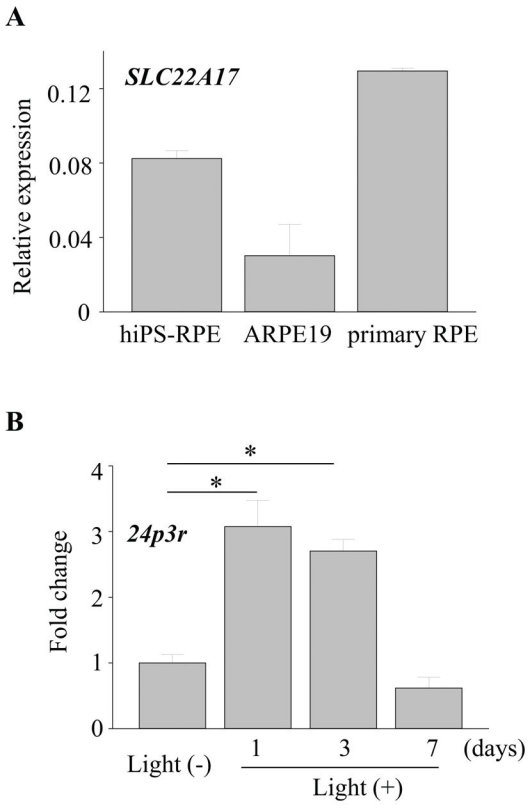

Figure 10. Expression of LCN2 receptor in RPE cells

A. RNA was extracted from human RPE cells differentiated from induced pluripotent stem cells (hiPS-RPE), ARPE19 (a human RPE derived cell line) and human primary RPE cells. Expression of *SLC22A17* was examined. Error bars indicate S.D. of the means, n=6. **B.** *Abca4*$^{-/-}$*Rdh8*$^{-/-}$ mice (1-month-old) were exposed to light at 10,000 lux for 30 min. RNA was extracted from RPE cells at different times points after light exposure. Expression levels of *24p3r* are presented as fold induction over non-light exposed control. Error bars indicate S.D. of the means, n=3, *$p < 0.05$.

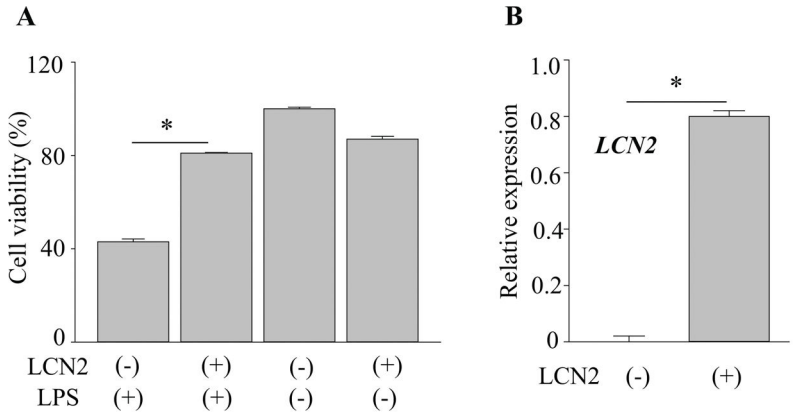

Figure 11. Overexpression of LCN2 in ARPE19 cells preserved cell viability against LPS-induced cell death

A. ARPE19 cells were transfected with *LCN2* in pcDNA3 vector. These cells were cultured with 1 μg/ml of LPS for 24 h, and cell viability was examined using WST-1 assay. Error bars indicate S.D. of the means, n=3, *$p < 0.05$. **B.** *LCN2* expression in transfected ARPE19 cells was quantified by qRT-PCR. Error bars indicate S.D. of the means, n=3, *$p < 0.05$.

Table 1

Fold changes in differentially expressed genes in Lcn2$^{-/-}$Abca4$^{-/-}$Rdh8$^{-/-}$ vs Abca4$^{-/-}$Rdh8$^{-/-}$ mice 24 h after light exposure.

Gene symbols	Gene names	Log2 fold change 24 h after light	p value
Upregulated Chemokines (C-C)			
CCL8	Chemokine (C-C motif) ligand 8	27.78	1.28E-21
CCL20	Chemokine (C-C motif) ligand 20	6.45	1.5E-21
CCL5	Chemokine (C-C motif) ligand 5	4.55	4.06E-21
CCL4	Chemokine (C-C motif) ligand 4	2.96	4.1E-21
CCL6	Chemokine (C-C motif) ligand 6	2.47	1.11E-20
CCL2	Chemokine (C-C motif) ligand 2	2.45	1.17E-20
CCL17	Chemokine (C-C motif) ligand 17	2.07	2.41E-20
Chemokines (C-X-C)			
CXCL5	Chemokine (C-C motif) ligand 5	17.21	2.96E-20
CXCL13	Chemokine (C-C motif) ligand 13	10.60	4.84E-20
CXCL10	Chemokine (C-C motif) ligand 10	3.02	5.26E-20
CXCL1	Chemokine (C-C motif) ligand 1	2.52	6.54E-20
Chemokine receptors			
CCR1	C-C motif Chemokine Receptor 1	10.60	7.96E-20
CCR5	C-C motif Chemokine Receptor 5	4.39	8.96E-20
CCR10	C-C motif Chemokine Receptor 10	2.48	8.6E-19
Interleukins/ receptors			
SPP1	Secreted phosphoprotein 1	6.99	5.87E-19
IL1A	Interleukin 1 alpha	4.77	1.66E-18
IL10	Interleukin 10	4.04	3.83E-18
MIF	Macrophage inhibitory factor	3.49	1.11E-17
TNF	Tumor necrosis factor	2.76	1.42E-17
IL1	Interleukin 1	2.52	5.42E-17
IL15	Interleukin 15	2.50	2.42E-17
IL2	Interleukin 2	2.38	3.42E-16
Downregulated			
CX3CL1	Chemokine (C-X3-C motif) ligand 1	-4.06	1.42E-17
VEGFA	Vascular Endothelial Growth Factor A	-3.84	3.42E-17
CXCL15	Chemokine (C-C motif) ligand 15	-2.22	5.42E-19

Significantly expressed genes ($p < 0.05$; fold changes ≥ 2.0) are listed. Minus signs (-) indicate reduced expression.

Table 2

Fold changes in differentially expressed microRNA genes in *Lcn2*$^{-/-}$ mice vs wild type mice 24 h after light exposure.

Gene symbols	Functional grouping of genes	Log2 fold change 24 h after light	p value
miR-429-3p	*Gpr68, Hmgb3, Il13, Ntf3, Prkca, Ripk2, Vegfa*	9.06	5.63E-57
let-7a-5p	*Casp3, Ccr7, Fgf11, Fgf5, Gdf6, Il13, Masp1*	7.01	2.67E-55
let-7b-5p	*Casp3, Ccr7, Fgf11, Fgf5, Gdf6, Il13*	7.01	2.00E-53
let-7e-5p	*Casp3, Ccr7, Fgf11, Fgf5, Gdf6, Il13*	7.01	5.24E-47
let-7f-5p	*Casp3, Ccr7, Fgf11, Fgf5, Gdf6, Il13, Masp*	7.01	6.42E-47
miR-1192	*Atrn, Bcl11a, Clcf1, Cyp26b1, Fgf7, Ptpra*	7.01	2.68E-45
miR-135a-5p	*Fgf11, Nampt, Sdcbp, Sp3, Tnfsf4, Txndc5*	7.01	2.84E-45
miR-140-5p	*Bmp2, Fgf9, Hdac4, Hdac7, Rac1, Spred1*	7.01	2.92E-45
miR-144-3p	*Cxcl12, Eda, Gdf10, Lifr, Ptgs2, Tnfsf11, Ttn*	7.01	3.87E-45
miR-155-5p	*Cebpb, Cyp26b1, Fgf7, Gdf6, Ms4a1, Sdcbp*	7.01	5.34E-44
miR-15a-5p	*Cd28, Eda, Fgf7, Ghr, Ifnk, Il10ra, Pik3r1*	7.01	9.51E-61
miR-186-5p	*Cast, Cntnap2, Cxcl13, Gdf6, Il13ra1, Pdgfc*	7.01	9.02E-59
miR-19a-3p	*Cast, Cbfb, Chst1, Cntfr, Cxcl12, F3, Impdh1*	7.01	1.01E-56
miR-19b-3p	*Cast, Cbfb, Chst1, Cntfr, Cxcl12, F3, Impdh1*	7.01	3.54E-50
miR-20a-5p	*F3, Mgll, Mink1, Osm, Pdcd1lg2, Ptger3, Stat3*	7.01	5.42E-50
miR-20b-5p	*F3, Mgll, Mink1, Osm, Pdcd1lg2, Ptger3, Stat3*	7.01	2.72E-48
miR-26b-5p	*Cmtm4, Inhbb, Pawr, Ppp3cb, Prkcd, Prkcq*	7.01	3.36E-48
miR-291a-3p	*Bcl11a, Bcl6, Cdkn1a, Cyp26b1, Dock2, F3*	7.01	3.94E-48
miR-294-3p	*Bcl11a, Bcl6, Cdkn1a, Cyp26b1, Dock2, F3*	7.01	5.88E-48
miR-295-3p	*Bcl11a, Bcl6, Cdkn1a, Cyp26b1, Dock2, F3*	7.01	9.03E-47
miR-29b-3p	*Atrn, Bcl11a, Hdac4, Il1rap, Lif, Pdgfc, Tnfrsf1a*	7.01	2.84E-46
miR-29c-3p	*Atrn, Bcl11a, Hdac4, Il1rap, Lif, Pdgfc, Tnfrsf1a*	7.01	5.88E-47
miR-301a-3p	*Cast, Cbfb, Chst1, Eda, Erbb2ip, Hprt1, Impdh1*	7.01	5.63E-52
miR-301b-3p	*Cast, Cbfb, Chst1, Eda, Erbb2ip, Hprt1, Impdh1*	7.01	2.67E-55
miR-302b-3p	*Bcl11a, Bcl6, Cdkn1a, Cyp26b1, Dock2, F3*	7.01	2.00E-53
miR-302d-3p	*Cd28, Eda, Fgf7, Ghr, Ifnk, Il10ra, Pik3r1*	7.01	5.24E-49
miR-322-5p	*Cd28, Eda, Fgf7, Ghr, Ifnk, Il10ra, Pik3r1*	7.01	6.42E-47
miR-325-3p	*Bcl11a, Bmi1, Cast, Cmtm6, Cntnap2, Cyp26b1*	7.01	2.68E-45
miR-340-5p	*Bcl11a, Bmi1, Cast, Cmtm6, Cntnap2, Cyp26b1*	7.01	5.88E-48
miR-106b-5p	*Atrn, Bmp3, Bmp4, Cd40lg, Chst2, Gfra2*	6.36	1.01E-56
miR-466d-3p	*Cast, Cbfb, Chst1, Eda, Erbb2ip, Hprt1, Impdh1*	4.79	2.72E-48
miR-669k-3p	*Cast, Cbfb, Chst1, Eda, Erbb2ip, Hprt1, Tnf*	4.03	5.63E-57
miR-130b-3p	*Cast, Cbfb, Chst1, Eda, Erbb2ip, Hprt1, Impdh1*	3.63	2.67E-55
miR-16-5p	*Cd28, Eda, Fgf7, Ghr, Ifnk, Il10ra, Pik3r1, Spr*	3.18	2.00E-53
miR-23a-3p	*Btla, Ccl7, Cxcl12, Erbb2ip, Fas, Grem1*	2.95	5.24E-47
let-7g-5p	*Casp3, Ccr7, Fgf11, Fgf5, Gdf6, Il13*	2.81	6.42E-47

Gene symbols	Functional grouping of genes	Log2 fold change 24 h after light	p value
miR-350-3p	*Cntnap2, Cyp26b1, Ghr, Il1rap, Il1m*	2.57	2.68E-45
miR-23b-3p	*Btla, Ccl7, Cxcl12, Erbb2ip, Fas, Grem1*	2.43	1.01E-58
miR-181a-5p	*Cd4, Il1a, Il7, Lif, Phf20l1, Prkcd, Tnf*	2.25	5.42E-51
miR-126a-5p	*Ap3b1, Cast, Cntnap2, Fgf7, Gfra2, Hdac4*	2.2	2.72E-49
miR-181c-5p	*Cd4, Il1a, Il7, Lif, Phf20l1, Prkcd, Tnf*	2.2	3.36E-48
miR-9-5p	*Ap3b1, Cmtm6, Cxcl11, Hdac5, Inhbb, Pdgfc*	2.19	3.94E-49
miR-30e-5p	*Cbfb, Chst1, Chst2, Hdac9, Hipk2*	2.1	9.03E-40
miR-200c-3p	*Gpr68, Hmgb3, Il13, Ntf3, Prkca, Ripk2, Vegfa*	2.06	3.36E-48

Significantly expressed genes ($p < 0.05$; fold changes ≥ 2.0) are listed.